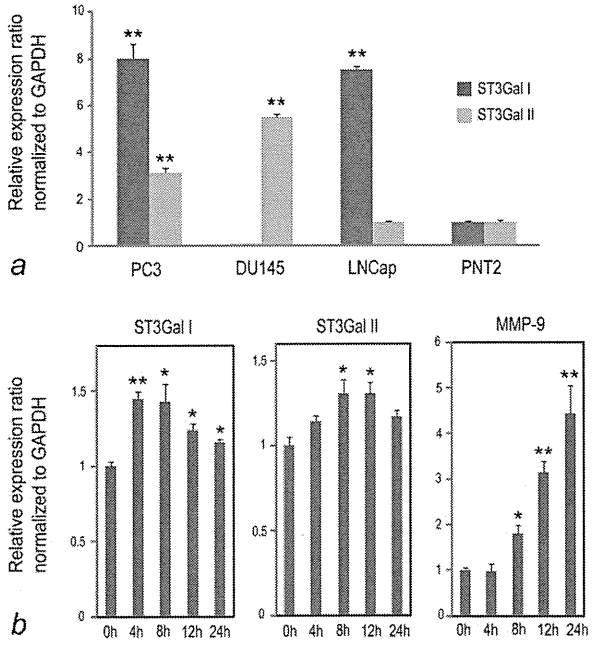

Figure 1. Expression of ST3Gal I and ST3Gal II in prostate cancer cells and normal prostate epithelium. (*a*) Quantitative real-time PCR analyses for ST3Gal I and ST3Gal II were performed on transcripts isolated from PC3, DU145, LNCap, and PNT2 cells. Expression is presented as the mean ± S.E. ($n = 3$) of the mRNA fold difference by normalizing with the expression level of PNT2 cells. $^{**}p < 0.001$. (*b*) PC3 cells were starved for 24 h in serum-free medium and then treated with 50 nM PMA for the indicated times. Quantitative real-time PCR analyses for ST3Gal I and ST3Gal II were performed, and expression is reported as the mean ± S.E. ($n = 3$) of the mRNA fold difference by normalizing with the expression level of PMA-untreated cells. MMP-9 was used as a positive control for PMA stimulation. $^{*}p < 0.05$, $^{**}p < 0.001$.

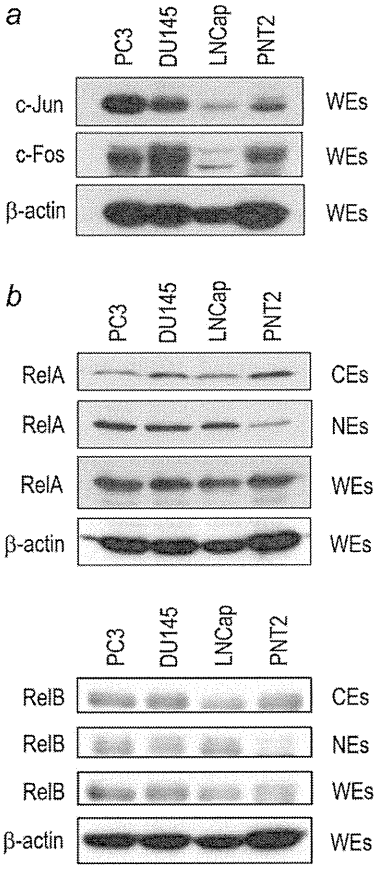

Figure 2. AP-1 and NF-κB are constitutively activated in castration-resistant prostate cancer cells. (*a*) Whole cell extracts (WEs) were prepared from PC3, DU145, LNCap, and PNT2 cells using a RIPA lysis buffer. Western blot analyses were performed with the indicated antibodies to detect c-Jun or c-Fos. β-actin was used as a control for protein loading. (*b*) Nuclear extracts (NEs) and cytoplasmic extracts (CEs) were prepared from PC3, DU145, LNCap, and PNT2 cells using NE-PER extraction reagents. Western blot analyses were performed with the indicated antibodies to detect RelA or RelB. β-actin was used as a control for protein loading.

1 transcription factors c-Jun and c-Fos can form a heterodimeric complex or a homodimeric c-Jun complex to regulate gene expression.[32] AP-1 transcription factors are associated with the progression and recurrence of prostate cancer.[33] To examine whether c-Jun and c-Fos are constitutively activated in prostate cancer cells, we performed western blot analyses with protein extracts from PC3, DU145, LNCap, and PNT2 cells (Fig. 2*a*). The expression of c-Jun and c-Fos was much higher in the castration-resistant prostate cancer cell lines, PC3 and DU145, than in the LNCap and PNT2 cells.

NF-κB transcription factors are also constitutively activated in prostate cancer cells[34,35] and up-regulated in metastatic castration-resistant prostate cancer cells.[36,37] To examine the activation of NF-κB transcription factors, RelA and RelB, in prostate cancer cells, we performed western blot analyses with protein extracts from PC3, DU145, LNCap, and PNT2 cells (Fig. 2*b*). Although western blot analyses of whole cell extracts did not reveal any significant change in the level of expression of RelA or RelB in all cells examined, the expression of RelA and RelB in the nucleus was much higher in prostate cancer cells, PC3, DU145, and LNCap, than in normal prostate epithelial cells, PNT2.

Inhibitory effects of NF-κB decoy ODN on PMA-induced ST3Gal I and ST3Gal II expression

To determine whether the transcriptional regulation of ST3Gal I and II is dependent on AP-1 or NF-κB, we first examined the inhibitory effects of AP-1 decoy ODN on PMA-induced ST3Gal I and II expression. To test the efficacy of AP-1 decoy ODN in PC3 cells, PC3 cells were co-transfected with AP-1 luciferase reporter gene and 1.0 μM decoy ODN for AP-1 or mutant decoy ODN and incubated in serum-free medium for 48 h. AP-1 decoy ODN significantly

inhibited the luciferase expression controlled by AP-1 in PC3 cells (Supporting Information Fig. 1). Then, PC3 cells were transfected with 1.0 μM decoy ODN for AP-1 or mutant decoy ODN. PC3 cells were incubated in serum-free medium for 48 h and treated with 50 nM PMA for up to 24 h. Quantitative real-time PCR analyses showed that PMA-induced ST3Gal I and II expression was not inhibited by AP-1 decoy ODN (Fig. 3*a*). When c-Jun siRNA was used to knock-down the expression of c-Jun in PC3 cells, no significant decrease in the expression of ST3Gal I and II was detected (Supporting Information Fig. 2). Thus, the transcriptional regulation of ST3Gal I and II did not seem to be AP-1-dependent.

Next, we examined the inhibitory effect of NF-κB decoy ODN on PMA-induced ST3Gal I and ST3Gal II expression (Fig. 3*b*). PC3 cells were transfected with 1.0 μM decoy ODN for NF-κB or scramble decoy ODN. PC3 cells were incubated in serum-free medium for 48 h and then treated with 50 nM PMA for up to 24 h. Quantitative real-time PCR analysis showed that PMA-induced ST3Gal I and ST3Gal II expression was inhibited by NF-κB decoy ODN. Thus, the transcriptional regulation of ST3Gal I and ST3Gal II seemed to be dependent on NF-κB.

Inhibitory effects of siRNA for RelA and RelB on expression of ST3Gal I and ST3Gal II

The NF-κB family is composed of five mammalian homologs, RelA (p65), RelB, c-Rel, p50 (NF-κB1) and p52 (NF-κB2), which form an array of homo- and hetero-dimers.[34] To identify the homologs that activate the expression of ST3Gal I and ST3Gal II, the inhibitory effects of siRNA for RelA, RelB, c-Rel, NF-κB1, or NF-κB2 on the expression of ST3Gal I and ST3Gal II were examined. In all the experiments using siRNA, cells were not treated with PMA. PC3 cells were transfected with either scramble RNA or siRNA for RelA, RelB, c-Rel, NF-κB1, or NF-κB2 and incubated for 72 h. The efficacy of RNAi was assessed by quantitative real-time PCR analyses (Supporting Information Fig. 3A). The protein level of RelA and RelB was also assessed by western blot analyses (Supporting Information Fig. 3B). Next, PC3 cells were transfected with either scramble RNA or siRNA for RelA, RelB, c-Rel, NF-κB1 or NF-κB2 and incubated for 72 h, and quantitative real-time PCR analyses of ST3Gal I and ST3Gal II were performed (Fig. 4). RelB siRNA suppressed the expression of both ST3Gal I and ST3Gal II, but RelA siRNA only inhibited the expression of ST3Gal II. Additionally, the inhibitory effect of RelA siRNA on ST3Gal II was smaller than that of RelB siRNA. SiRNA for c-Rel, NF-κB1, and NF-κB2 did not significantly change the expression of ST3Gal I and II. Among the five mammalian homologs of the NF-κB family, RelB RNAi most effectively inhibited the expression of ST3Gal I and II in PC3 cells. Among castration-resistant prostate cancer cells, DU145 cells also produced greater amounts of ST3Gal II as shown in Figure 1. We examined the inhibitory effects of RelB siRNA on expression of ST3Gal II in DU145 cells. RelB RNAi also suppressed the expression of ST3Gal II in DU145 cells (Supporting Information Fig. 4).

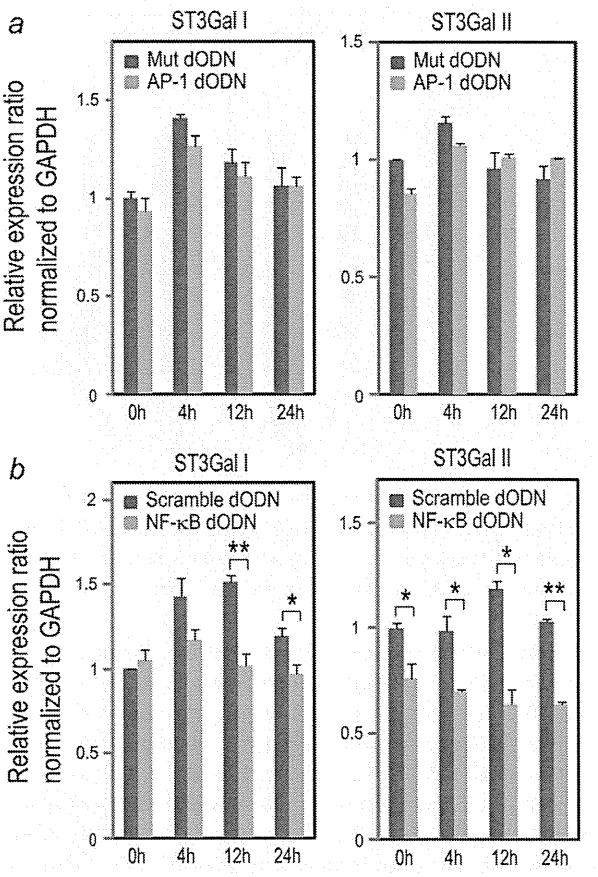

Figure 3. Inhibitory effects of AP-1 or NF-κB decoy ODN on PMA-induced ST3Gal I and ST3Gal II expression. (*a*) PC3 cells were transfected with 1.0 μM decoy ODN for AP-1 (AP-1 dODN) or corresponding mutant decoy ODN (Mut dODN). PC3 cells were incubated in serum-free medium for 48 h and then treated with 50 nM PMA for the indicated times. Quantitative real-time PCR analyses for ST3Gal I and ST3Gal II were performed, and expression is reported as the mean ± S.E. ($n = 3$) of the mRNA fold difference by normalizing with the expression level of mutant decoy–transfected and PMA-untreated cells. (*b*) PC3 cells were transfected with 1.0 μM decoy ODN for NF-κB (NF-κB dODN) or corresponding scramble decoy ODN (Scramble dODN). PC3 cells were incubated in serum-free medium for 48 h and then treated with 50 nM PMA for the indicated times. Quantitative real-time PCR analyses for ST3Gal I and ST3Gal II were performed, and expression is reported as the mean ± S.E. ($n = 3$) of the mRNA fold difference by normalizing with the expression level of scramble decoy–transfected and PMA-untreated cells. *$p < 0.05$, **$p < 0.001$.

NF-κB–dependent transcriptional regulation of ST3Gal VI

The expression of SPG was up-regulated in castration-resistant prostate cancer cells.[7] SPG is synthesized from neolactotetraosylceramide by ST3Gal VI.[19,23] We determined the constitutive expression level of ST3Gal VI in prostate cancer

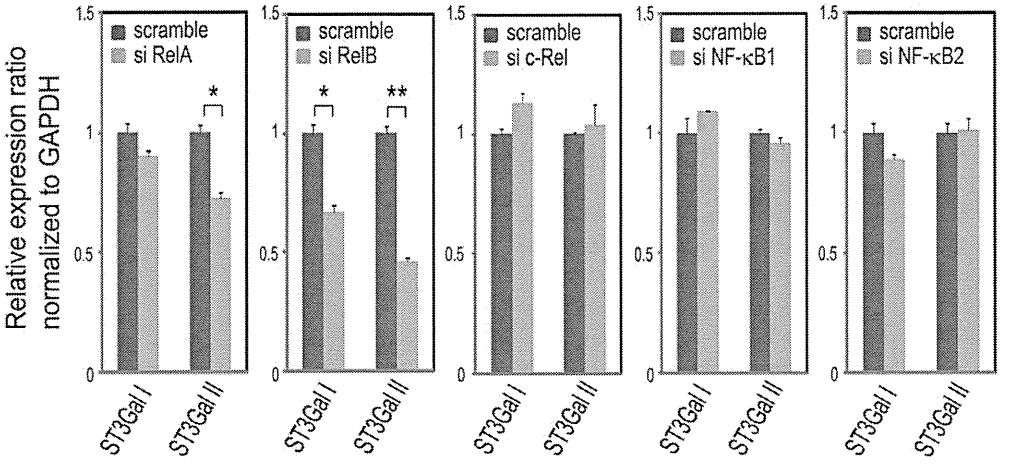

Figure 4. Inhibitory effects of siRNA for RelA and RelB on expression of ST3Gal I and ST3Gal II. PC3 cells were transfected with either scramble RNA or siRNA for RelA, RelB, c-Rel, NFκ-B1, or NFκ-B2 and incubated for 72 h. Quantitative real-time PCR analyses for ST3Gal I and ST3Gal II were performed, and expression is reported as the mean ± S.E. ($n = 3$) of the mRNA fold difference by normalizing with the expression level of scramble RNA–transfected cells. *$p < 0.05$, **$p < 0.001$.

cells and normal prostate epithelium using quantitative real-time PCR (Fig. 5*a*). Castration-resistant prostate cancer cell lines, PC3 and DU145, produced greater amounts of ST3Gal VI than LNCap and PNT2. Next, we examined whether the expression of ST3Gal VI is induced by PMA. PC3 cells were starved for 24 h in serum-free medium and then treated with 50 nM PMA for up to 24 h. Quantitative real-time PCR analysis showed that the expression of ST3Gal VI is induced by PMA (Supporting Information Fig. 5A). To determine whether the transcriptional regulation of ST3Gal VI is AP-1 dependent or NF-κB dependent, the inhibitory effects of AP-1 decoy ODN or NF-κB decoy ODN on PMA-induced ST3Gal VI expression were examined (Supporting Information Fig. 5B). Quantitative real-time PCR analyses showed that PMA-induced ST3Gal VI expression was inhibited by NF-κB decoy ODN, not by AP-1 decoy ODN. Thus, transcriptional regulation of ST3Gal VI seems to be NF-κB-dependent. To identify the homologs of the NF-κB family that activate the expression of ST3Gal VI, the inhibitory effects of siRNA for RelA, RelB, c-Rel, NF-κB1 or NF-κB2 on the expression of ST3Gal VI were examined (Fig. 5*b*). SiRNA for RelA and RelB inhibited the expression of ST3Gal VI, while siRNA for c-Rel, NF-κB1, and NF-κB2 did not change the expression level. Among the five mammalian homologs of the NF-κB family, RelB RNAi was also the most effective inhibitor of ST3Gal VI expression, as shown above.

Inhibitory effects of RelB siRNA on the expression of GD1a and SPG

Our results suggested that RelB could regulate the production of GD1a and SPG in PC3 cells by the transcriptional control of ST3Gal I, ST3Gal II, and ST3Gal VI. Therefore, we examined the effect of RelB siRNA on the production of ganglioside GD1a and SPG using HPLC (Fig. 6). The amount of GD1a and SPG in PC3 cells was significantly reduced by RelB siRNA treatment.

Discussion

Here, we demonstrate that GD1a production is mediated by NF-κB, mainly RelB, through the transcriptional control of ST3Gal I and II, which synthesize GD1a from GM1.[38] NF-κB plays pivotal roles in cell survival, inflammation, innate immunity, adaptive immunity, and the development of secondary lymphoid organs.[39] NF-κB signaling is also involved in the progression of various cancers.[39] The activation of AP-1[33] and NF-κB[34,35] is involved in the growth and progression of prostate cancers. Our results show that GD1a production in castration-resistant prostate cancer cells is regulated by NF-κB, not by AP-1. Accordingly, this is the first report to suggest the contribution of NF-κB in the growth and progression of prostate cancers *via* ganglioside production.

SPG, a neolacto-series ganglioside, is synthesized by ST3Gal VI.[19,23] Previously, we reported that SPG was abundantly produced in castration-resistant prostate cancer cells, PC3 and DU145.[7] However, the biological function of SPG has not been identified. In the present report, ST3Gal VI was up-regulated by NF-κB signaling. Therefore, we speculate that SPG might play a role in promoting the growth and progression of prostate cancers.

Genes for human ST3Gal I, II, and VI were cloned,[40–42] and their promoter sequences were available in public. NF-κB binding sites have been found in ST3Gal I[43] but not in ST3Gal II and VI. We searched for putative NF-κB binding sites in the region necessary for active transcription of ST3Gal II (−801 to −660 of p1 promoter) and ST3Gal VI (p2 promoter) in PC3 cells.[41,42] Based on previous reports,[44,45] we used 5′-GGGRNWYYCC-3′ (R; purine, Y; pyrimidine, W; A or T and

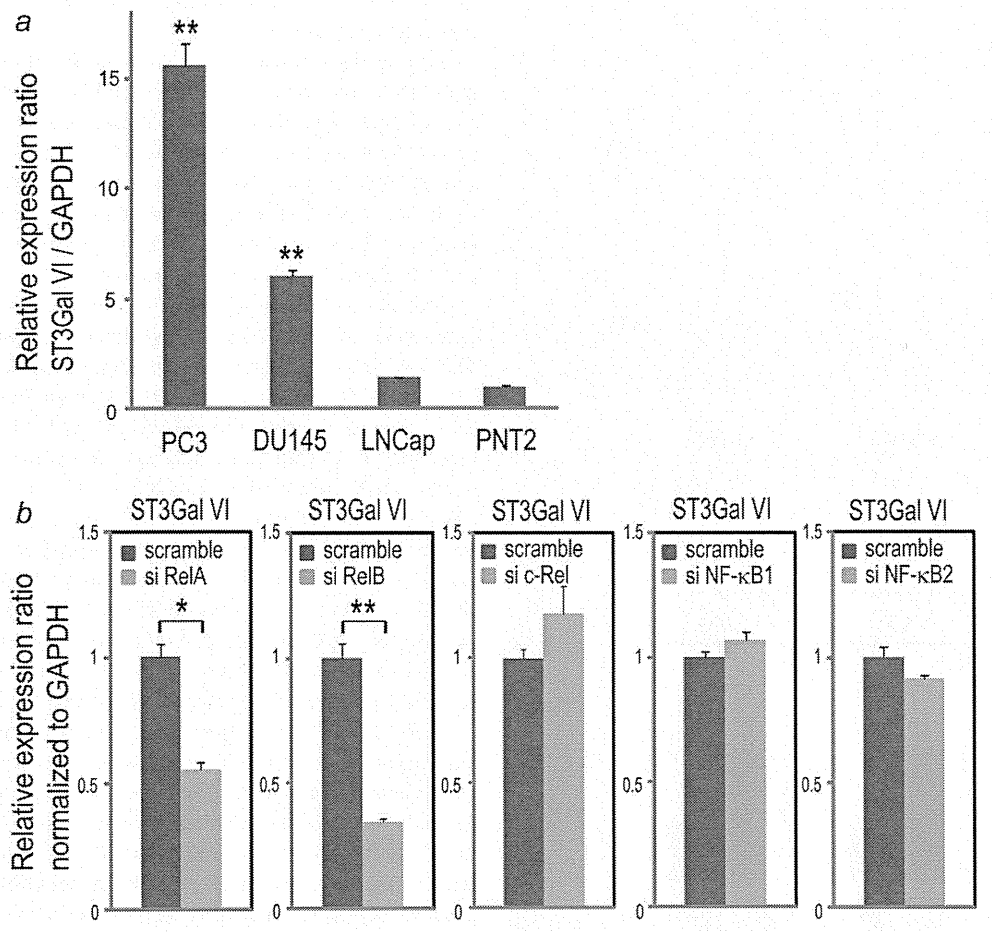

Figure 5. NF-κB-dependent transcriptional regulation of ST3Gal VI. (*a*) Expression of ST3Gal VI in prostate cancer cells and normal prostate epithelium. Quantitative real-time PCR analysis for ST3Gal VI was performed on transcripts isolated from PC3, DU145, LNCap, and PNT2 cells. Expression is reported as the mean ± S.E. ($n = 3$) mRNA fold difference after normalizing to the expression level of PNT2 cells. (*b*) Inhibitory effects of siRNA of RelA and RelB on the expression of ST3Gal VI. PC3 cells were transfected with either scramble RNA or siRNA for RelA, RelB, c-Rel, NF-κB1 or NF-κB2 and incubated for 72 h. Quantitative real-time PCR analyses for ST3Gal VI were performed, and the expression is reported as the mean ± S.E. ($n = 3$) of the mRNA fold difference by normalizing to the expression level of scramble RNA–transfected cells. *$p < 0.05$, **$p < 0.001$.

N; any nucleotide) as the consensus sequence for NF-κB binding. One putative site for NF-κB (RelA and RelB) was found in ST3Gal II (−792 to −783) and ST3Gal VI (−914 to −905). This is the first report to suggest the contribution of NF-κB, mainly of RelB, in the transcriptional regulation of ST3Gal II and ST3Gal VI in human castration-resistant prostate cancer cells. The report of NF-κB binding sites in ST3Gal I indicates that NF-κB-p65 (RelA) regulates ST3Gal I expression in human colon adenocarcinoma HT-29.[43] Although the authors did not test the effect of NF-κB components other than RelA on ST3Gal I expression, the NF-κB component that predominantly affects ST3Gal transcription may be different among various cancers.

The activation of NF-κB signaling in prostate cancers is caused by the loss of PTEN function[46] or p53 mutation.[47] The loss of p53 function occurs in PC3 and DU145 cells,[48] while PTEN deficiency occurs in PC3 and LNCap cells.[49] Thus, NF-κB signaling is highly activated in these prostate cancer cell lines (as shown in Fig. 2). The two routes in NF-κB signaling are the canonical pathway, which involves the complex of RelA and p50, and the non-canonical pathway, which involves the complex of RelB and p52.[39] Western blot analyses (Fig. 2) revealed that both RelA and RelB were activated in PC3 cells. It was reported that RelB binding sites in the promoter region are also recognized by RelA.[45] Therefore, both RelA and RelB should contribute to the expression of ST3Gal I, II and VI. Actually, both RelA siRNA and RelB siRNA suppressed the expression of ST3Gal II and VI. However, RelB siRNA mediated more effective inhibition as compared to RelA siRNA. This difference may be due to the expression level of RelA and RelB in the nucleus of PC3 cells,

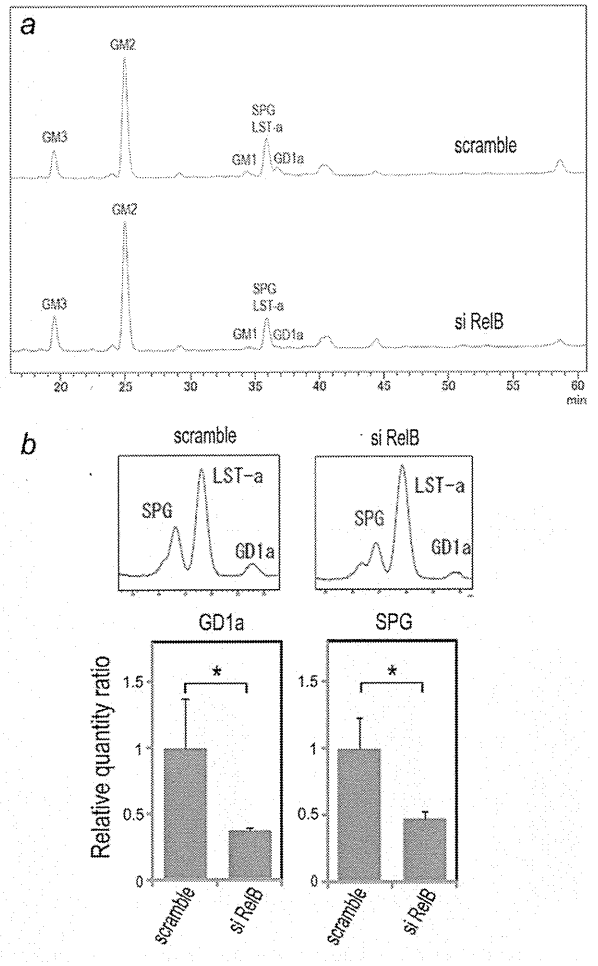

Figure 6. Inhibitory effects of RelB siRNA on the expression of GD1a and SPG. (*a*) PC3 cells were transfected with either RelB siRNA or scramble RNA and incubated for 120 h. The acidic GSLs of PC3 cells were separated by molecular size of oligosaccharides using normal-phase HPLC. (*b*) Peaks containing SPG, LST-a and GD1a were further purified by reversed-phase HPLC. The quantity of GD1a and SPG was determined by the total area size of those 2 gangliosides and is reported as the mean ± S.E. ($n = 3$) of the fold difference by normalizing with the quantity of scramble RNA–transfected cells. *$p < 0.05$. [Color figure can be viewed in the online issue, which is available at wileyonlinelibrary.com.]

as RelB is expressed more abundantly than RelA in the nuclei of prostate cancer tissues with higher Gleason scores.[35] Recently, the involvement of RelB in the enhanced growth of prostate cancers has also been reported.[50] Thus, RelB may play a dominant role in transcriptional regulation in castration-resistant prostate cancers.

Among the five mammalian homologs of the NF-κB family, RelB RNAi was the most effective inhibitor for ST3Gal I, II, and VI expression. However, the almost complete down regulation of RelB resulted in about 50-60% inhibition of ST3Gal II and VI (Figs. 4 and 5). There was relative little effect on ST3Gal I (Fig. 4). These results suggest that transcriptional factors other than NF-κB are also involved in the expression of ST3Gal I, II, and VI, although RelB is a main regulator.

LNCap, a hormone-sensitive prostate cancer cell line, has scant levels of GD1a[7] despite high levels of ST3Gal I (Fig. 1). The low levels of GD1a are presumably caused by the low levels of GM1, (from which GD1a is synthesized) in LNCaP cells.[7] It is interesting that ST3Gal II and VI were not up-regulated in LNCap cells, although comparable amounts of nuclear RelB were present in LNCap, PC3, and DU145 cells (Fig. 2). We are currently analyzing the mechanism of transcriptional regulation of these sialyltransferases in LNCap cells. The expression of ST3Gal I was inhibited by RelB siRNA, however the expression of ST3Gal II and VI was not affected by RelB siRNA in LNCap cells (data not shown). Epigenetic regulations, such as DNA methylation and histone modifications, might be responsible for this regulation.

Many cancer cells frequently express high amounts of sialylated glycans on their surface,[13] which may promote cancer cell growth and invasion. Therefore, the sialyltransferases that produce these sialylated structures have received much attention.[13] In this study, we demonstrated that NF-κB is up-regulated in castration-resistant prostate cancer cells and the production of GD1a and SPG in castration-resistant prostate cancer cells was controlled by NF-κB, mainly by RelB, through the transcriptional regulation of ST3Gal I, II and VI. We previously reported that inactivated Sendai virus particles very efficiently infects castration-resistant human prostate cancer cell lines, PC3 and DU145, because of the high production of viral receptor gangliosides such as GD1a and SPG and selectively induced apoptosis in human castration-resistant prostate cancer cells by RIG-I–mediated gene expression,[7] in addition to the induction of multiple anti-tumor immunities.[7,8] The results reported here provide us with scientific explanation on the susceptibility of castration-resistant prostate cancer cells to inactivated Sendai virus particle. Based on those results, we are going to start a clinical trial to treat prostate cancers in patients using inactivated Sendai virus particle in 2011. The discovery of the involvement of RelB in the production of GD1a and SPG will also contribute to the clinical trial in the evaluation of the efficacy of inactivated Sendai virus particle.

References

1. Jemal A, Siegel R, Ward E, Hao Y, Xu J, Murray T, Thun MJ. Cancer statistics. *CA Cancer J Clin* 2008;58:71–96.
2. Isaacs JT. The biology of hormone refractory prostate cancer. Why does it develop? *Urol Clin North Am* 1999;26: 263–73.
3. Gulley J, Figg WD, Dahut WL. Treatment options for androgen-independent prostate cancer. *Clin Adv Hematol Oncol* 2003;1:49–57.
4. Freytag SO, Stricker H, Movsas B, Kim JH. Prostate cancer gene therapy clinical trials. *Mol Ther* 2007;15:1042–52.
5. Li X, Liu Y, Tang Y, Roger P, Jeng MH, Kao C. Docetaxel increases antitumor

efficacy of oncolytic prostate-restricted replicative adenovirus by enhancing cell killing and virus distribution. *J Gene Med* 2010;12:516–27.
6. Castelo-Branco P, Passer BJ, Buhrman JS, Antoszczyk S, Marinelli M, Zaupa C, Rabkin SD, Martuza RL. Oncolytic herpes simplex virus armed with xenogeneic homologue of prostatic acid phosphatase enhances antitumor efficacy in prostate cancer. *Gene Ther* 2010;17:805–10.
7. Kawaguchi Y, Miyamoto Y, Inoue T, Kaneda Y. Efficient eradication of hormone-resistant human prostate cancers by inactivated Sendai virus particle. *Int J Cancer* 2009;124:2478–87.
8. Kurooka M, Kaneda Y. Inactivated Sendai virus particles eradicate tumors by inducing immune responses through blocking regulatory T cells. *Cancer Res* 2007;1:227–36.
9. Villar E, Barroso IM. Role of sialic acid-containing molecules in paramyxovirus entry into the host cell: a minireview. *Glycoconj J* 2006;23:5–17.
10. Ravindranath MH, Muthugounder S, Presser N, Selvan SR, Portoukalian J, Brosman S, Morton DL. Gangliosides of organ-confined versus metastatic androgen-receptor-negative prostate cancer. *Biochem Biophys Res Commun* 2004;324:154–65.
11. Ravindranath MH, Muthugounder S, Presser N, Ye X, Brosman S, Morton DL. Endogenous immune response to gangliosides in patients with confined prostate cancer. *Int J Cancer* 2005;116: 368–77.
12. Yamashita T, Wada R, Sasaki T, Deng C, Bierfreund U, Sandhoff K, Proia RL. A vital role for glycosphingolipid synthesis during development and differentiation. *Proc Natl Acad Sci U S A* 1999;96:9142–7.
13. Hakomori S. Tumor malignancy defined by aberrant glycosylation and sphingo(glyco)lipid metabolism. *Cancer Res* 1996;56:5309–18.
14. Taki T, Ishikawa D, Ogura M, Nakajima M, Handa S. Ganglioside GD1alpha functions in the adhesion of metastatic tumor cells to endothelial cells of the target tissue. *Cancer Res* 1997;57:1882–8.
15. Li R, Liu Y, Ladisch S. Enhancement of epidermal growth factor signaling and activation of SRC kinase by gangliosides. *J Biol Chem* 2001;276:42782–92.
16. Lang Z, Guerrera M, Li R, Ladisch S. Ganglioside GD1a enhances VEGF-induced endothelial cell proliferation and migration. *Biochem Biophys Res Commun* 2001;282: 1031–7.
17. Liu Y, Li R, Ladisch S. Exogenous ganglioside GD1a enhances epidermal growth factor receptor binding and dimerization. *J Biol Chem* 2004;279: 36481–9.
18. Kanda T, Ariga T, Kubodera H, Jin HL, Owada K, Kasama T, Yamawaki M, Mizusawa H. Glycosphingolipid composition of primary cultured human brain microvascular endothelial cells. *J Neurosci Res* 2004;78:141–50.
19. Takashima S. Characterization of mouse sialyltransferase genes: their evolution and diversity. *Biosci Biotechnol Biochem* 2008; 72:1155–67.
20. Lee YC, Kojima N, Wada E, Kurosawa N, Nakaoka T, Hamamoto T, Tsuji S. Cloning and expression of cDNA for a new type of Gal beta 1,3GalNAc alpha 2,3-sialyltransferase. *J Biol Chem* 1994;269: 10028–33.
21. Kojima N, Lee YC, Hamamoto T, Kurosawa N, Tsuji S. Kinetic properties and acceptor substrate preferences of two kinds of Gal beta 1,3GalNAc alpha 2,3-sialyltransferase from mouse brain. *Biochemistry* 1994;33:5772–6.
22. Kono M, Ohyama Y, Lee YC, Hamamoto T, Kojima N, Tsuji S. Mouse beta-galactoside alpha 2,3-sialyltransferases: comparison of in vitro substrate specificities and tissue specific expression. *Glycobiology* 1997;7:469–79.
23. Okajima T, Fukumoto S, Miyazaki H, Ishida H, Kiso M, Furukawa K, Urano T, Furukawa K. Molecular cloning of a novel alpha2,3-sialyltransferase (ST3Gal VI) that sialylates type II lactosamine structures on glycoproteins and glycolipids. *J Biol Chem* 1999;274:11479–86.
24. Videira PA, Correia M, Malagolini N, Crespo HJ, Ligeiro D, Calais FM, Trindade H, Dall'Olio F. ST3Gal.I sialyltransferase relevance in bladder cancer tissues and cell lines. *BMC Cancer* 2009;9:357.
25. Saito S, Aoki H, Ito A, Ueno S, Wada T, Mitsuzuka K, Satoh M, Arai Y, Miyagi T. Human alpha2,3-sialyltransferase (ST3Gal II) is a stage-specific embryonic antigen-4 synthase. *J Biol Chem* 2003;278:26474–9.
26. Hölschermann H, Stadlbauer TH, Wagner AH, Fingerhuth H, Muth H, Rong S, Güler F, Tillmanns H, Hecker M. STAT-1 and AP-1 decoy oligonucleotide therapy delays acute rejection and prolongs cardiac allograft survival. *Cardiovasc Res* 2006;71: 527–36.
27. Morishita R, Sugimoto T, Aoki M, Kida I, Tomita N, Moriguchi A, Maeda K, Sawa Y, Kaneda Y, Higaki J, Ogihara T. In vivo transfection of cis element "decoy" against nuclear factor-kappaB binding site prevents myocardial infarction. *Nat Med* 1997;3: 894–9.
28. Korekane H, Tsuji S, Noura S, Ohue M, Sasaki Y, Imaoka S, Miyamoto Y. Novel fucogangliosides found in human colon adenocarcinoma tissues by means of glycomic analysis. *Anal Biochem* 2007;364: 37–50.
29. Weinberg RA, ed. The biology of cancer. New York: Garland Science, Taylor and Francis Group, 2007. 439 p.
30. Madigan MC, Kingsley EA, Cozzi PJ, Delprado WJ, Russell PJ, Li Y. The role of extracellular matrix metalloproteinase inducer protein in prostate cancer progression. *Cancer Immunol Immunother* 2008;57:1367–79.
31. Sato H, Kita M, Seiki M. v-Src activates the expression of 92-kDa type IV collagenase gene through the AP-1 site and the GT box homologous to retinoblastoma control elements. A mechanism regulating gene expression independent of that by inflammatory cytokines. *J Biol Chem* 1993; 268:23460–8.
32. Abate C, Curran T. Encounters with Fos and Jun on the road to AP-1. *Semin Cancer Biol* 1990;1:19–26.
33. Ouyang X, Jessen WJ, Al-Ahmadie H, Serio AM, Lin Y, Shih WJ, Reuter VE, Scardino PT, Shen MM, Aronow BJ, Vickers AJ, Gerald WL, et al. Activator protein-1 transcription factors are associated with progression and recurrence of prostate cancer. *Cancer Res* 2008;68: 2132–44.
34. Suh J, Rabson AB. NF-kappaB activation in human prostate cancer: important mediator or epiphenomenon? *J Cell Biochem* 2004;91:100–17.
35. Lessard L, Bégin LR, Gleave ME, Mes-Masson AM, Saad F. Nuclear localisation of nuclear factor-kappaB transcription factors in prostate cancer: an immunohistochemical study. *Br J Cancer* 2005;93:1019–23.
36. Jin RJ, Lho Y, Connelly L, Wang Y, Yu X, Saint Jean L, Case TC, Ellwood-Yen K, Sawyers CL, Bhowmick NA, Blackwell TS, Yull FE, et al. The nuclear factor-kappaB pathway controls the progression of prostate cancer to androgen-independent growth. *Cancer Res* 2008;68:6762–9.
37. Min J, Zaslavsky A, Fedele G, McLaughlin SK, Reczek EE, De Raedt T, Guney I, Strochlic DE, Macconaill LE, Beroukhim R, Bronson RT, Ryeom S, et al. An oncogene-tumor suppressor cascade drives metastatic prostate cancer by coordinately activating Ras and nuclear factor-kappaB. *Nat Med* 2010;16:286–94.
38. Tsuji S. Molecular cloning and functional analysis of sialyltransferases. *J Biochem* 1996;120:1–13.
39. Bollrath J, Greten FR. IKK/NF-kappaB and STAT3 pathways: central signaling hubs in inflammation-mediated tumour promotion and metastasis. *EMBO Rep* 2009;10:1314–9.
40. Taniguchi A, Yoshikawa I, Matsumoto K. Genomic structure and transcriptional regulation of human Galbeta1,3GalNAc alpha2,3-sialyltransferase (hST3Gal I) gene. *Glycobiology* 2001;11:241–7.

41. Taniguchi A, Morishima T, Tsujita Y, Matsumoto Y, Matsumoto K. Genomic structure, expression, and transcriptional regulation of human Gal beta 1,3 GalNAc alpha 2,3-sialyltransferase gene. *Biochem Biophys Res Commun* 2003;300:570–6.
42. Taniguchi A, Kaneta R, Morishita K, Matsumoto K. Gene structure and transcriptional regulation of human Gal beta1,4(3) GlcNAc alpha2,3-sialyltransferase VI (hST3Gal VI) gene in prostate cancer cell line. *Biochem Biophys Res Commun* 2001;287:1148–56.
43. Higai K, Ishihara S, Matsumoto K. NFkappaB-p65 dependent transcriptional regulation of glycosyltransferases in human colon adenocarcinoma HT-29 by stimulation with tumor necrosis factor alpha. *Biol Pharm Bull* 2006;29:2372–7.
44. Fusco AJ, Huang DB, Miller D, Wang VY, Vu D, Ghosh G. NF-kappaB p52:RelB heterodimer recognizes two classes of kappaB sites with two distinct modes. *EMBO Rep* 2009;10:152–9.
45. Britanova LV, Makeev VJ, Kuprash DV. In vitro selection of optimal RelB/p52 DNA-binding motifs. *Biochem Biophys Res Commun* 2008;365:583–8.
46. Uzoh CC, Perks CM, Bahl A, Holly JM, Sugiono M, Persad RA. PTEN-mediated pathways and their association with treatment-resistant prostate cancer. *BJU Int* 2009;104:556–61.
47. Meylan E, Dooley AL, Feldser DM, Shen L, Turk E, Ouyang C, Jacks T. Requirement for NF-kappaB signalling in a mouse model of lung adenocarcinoma. *Nature* 2009;462:104–7.
48. Cohen MB, Rokhlin OW. Mechanisms of prostate cancer cell survival after inhibition of AR expression. *J Cell Biochem* 2009;106:363–71.
49. Jiang X, Chen S, Asara JM, Balk SP. Phosphoinositide 3-kinase pathway activation in phosphate and tensin homolog (PTEN)-deficient prostate cancer cells is independent of receptor tyrosine kinases and mediated by the p110beta and p110delta catalytic subunits. *J Biol Chem* 2010;285:14980–9.
50. Xu Y, Josson S, Fang F, Oberley TD, St Clair DK, Wan XS, Sun Y, Bakthavatchalu V, Muthuswamy A, St Clair WH. RelB enhances prostate cancer growth: implications for the role of the nuclear factor-kappaB alternative pathway in tumorigenicity. *Cancer Res* 2009;69:3267–71.

JJCO Japanese Journal of Clinical Oncology

Jpn J Clin Oncol 2011;41(2)253–259
doi:10.1093/jjco/hyq178
Advance Access Publication 10 November 2010

Retrospective Analysis of an Oral Combination of Dexamethasone, Uracil plus Tegafur and Cyclophosphamide for Hormone-refractory Prostate Cancer

Koji Hatano[1], Norio Nonomura[1,*], Kazuo Nishimura[2], Atsunari Kawashima[1], Masatoshi Mukai[1], Akira Nagahara[1], Yasutomo Nakai[1], Masashi Nakayama[1], Hitoshi Takayama[1], Akira Tsujimura[1] and Akihiko Okuyama[1]

[1]Department of Urology, Osaka University Graduate School of Medicine, Suita and [2]Department of Urology, Osaka Medical Center for Cancer and Cardiovascular Diseases, Osaka Japan

*For reprints and all correspondence: Norio Nonomura, Department of Urology, Osaka University Graduate School of Medicine, 2-2 Yamadaoka, Suita 565-0871, Japan. E-mail: nono@uro.med.osaka-u.ac.jp

Received March 19, 2010; accepted August 27, 2010

Objective: To evaluate the clinical utility of an oral combination of dexamethasone, uracil plus tegafur and cyclophosphamide as a treatment for patients with hormone-refractory prostate cancer.
Methods: Fifty-seven patients with hormone-refractory prostate cancer were treated with an oral administration of dexamethasone (1.0 mg/day), uracil plus tegafur (400 mg/day) and cyclophosphamide (100 mg/day). The median patient age was 71 years. Sixteen patients had symptomatic bone metastasis, 31 had asymptomatic bone metastasis and 8 showed lymph node metastasis. Eight patients presented with only biochemical progression as evaluated by serum prostate-specific antigen levels.
Results: Thirty-six (63%) of 57 patients demonstrated a $\geq$50% decline in serum prostate-specific antigen levels. The median time to prostate-specific antigen progression was 7.2 months. In patients with a prostate-specific antigen decline of $\geq$50%, the median time to progression was 13.3 months. With respect to pre-treatment markers, the duration of response to initial hormonal treatment was associated with the time to prostate-specific antigen progression. In 11 of 16 (69%) patients who complained of bone pain, the pain improved and became stable in 5 of those patients (31%). Most adverse events were mild and only three (5%) patients showed neutropenia of Grade 3 or higher.
Conclusions: The combination of dexamethasone, uracil plus tegafur and cyclophosphamide is an effective and well tolerated regimen for hormone-refractory prostate cancer. To evaluate the survival benefits, further randomized studies are required.

Key words: chemotherapy cyclophosphamide – dexamethasone – hormone-refractory prostate cancer – UFT

INTRODUCTION

Male prostate cancer is the second leading cause of cancer in the USA (1) and is a growing problem worldwide. Most patients with advanced prostate cancer will respond to testicular androgen blockade, castration or use of a luteinizing hormone-releasing hormone (LHRH) analogue with or without antiandrogen. The median duration of response, however, is <2 years after initial hormonal therapy for these patients (2,3). Once the disease becomes hormone-refractory prostate cancer (HRPC), curing the patient becomes difficult. Docetaxel has been shown to prolong survival in patients with HRPC by about 2 months in Phase III trials (4,5). In the trial, 56% of patients showed toxicities of Grade 3 or higher in the docetaxel group (4).

The clinical efficacy of low doses of dexamethasone in the treatment of patients with HRPC has been reported

previously (6–11). Although subjective and objective response rates varied, definite effects in these patients have been documented in terms of decreased prostate-specific antigen (PSA) levels or palliative activity (6–11). The exact mechanisms underlying decreases in PSA levels by dexamethasone are unclear, although dexamethasone has been proposed to suppress adrenal androgen (12). In addition, anti-inflammatory effects may play a key role in the palliation of pain from bone metastases, and the *in vitro* and *in vivo* activity of dexamethasone against androgen-independent prostate cancer cell lines has been described (13–15). Low doses of dexamethasone have significant activity in HRPC with low toxicity and its potential for use in combination with novel agents has been reported (11).

UFT is a combination of tegafur and uracil. UFT, as a single agent, has been reported to be effective in treating patients with HRPC (16,17). Oral cyclophosphamide has also been validated against HRPC when used alone (18,19) and in combination with dexamethasone (20,21). In our previous study that examined oral combination therapy with cyclophosphamide, UFT and estramustine in patients with HRPC, 12 (57%) of 21 showed a ≥50% decline in PSA with minor toxicity (22). In the present study, we evaluated an oral combination composed of dexamethasone, UFT and cyclophosphamide as a treatment for patients with HRPC. The regimen was designed with the goal of easy administration in an outpatient setting and with the expectation of minimal toxicity for most patients with HRPC in view of their advanced age and poor physical condition.

PATIENTS AND METHODS

Patients

Fifty-seven patients with HRPC were treated with an oral combination of dexamethasone, UFT and cyclophosphamide at Osaka University Hospital from November 1996 to August 2008. Eligibility criteria included the following: HRPC, defined as serially increasing PSA values on three or more occasions at least 2 weeks apart or radiologically detected new or extensive lesions; a castration level of serum testosterone while receiving hormonal therapy; an Eastern Cooperative Oncology Group (ECOG) performance status of 2 or less; and a life expectancy of ≥3 months.

Pre-treatment characteristics of all patients are shown in Table 1. Patient age ranged from 49 to 90 years (median, 71 years). A bone scan, computed tomography (CT) or magnetic resonance imaging (MRI) was performed to evaluate the sites of metastatic diseases. Forty-seven patients had bone disease, eight had lymph node involvement and one had liver metastasis. In contrast, eight patients had only biochemical disease progression as evaluated by PSA. With respect to symptom status, 16 patients had bone pain due to metastasis.

Prior therapies are shown in Table 2. As a primary hormonal therapy, all patients received complete androgen blockade of medical or surgical castration plus an antiandrogen. The antiandrogen was discontinued at least 4 weeks before initiating this regimen or prior chemotherapy to observe the antiandrogen withdrawal response. Seventeen patients (30%) had demonstrated a decline in serum PSA after antiandrogen withdrawal (antiandrogen withdrawal syndrome). Chemotherapies were administered in 36 patients (63%) after disease progression subsequent to initial hormonal therapy. Estramustine-based chemotherapies were administered in 26 patients (46%), low doses of oral dexamethasone were administered in 25 patients (44%) and docetaxel was administered in 2 patients.

Treatment

The treatment regimen, which was applied on an outpatient basis, consisted of dexamethasone (1.0 mg/day), UFT (400 mg/day as a dose of tegafur) and cyclophosphamide (100 mg/day), all given orally in two daily fractions. Four patients, all of whom were 80 years of age or more, received dexamethasone (0.5 mg/day), UFT (200 mg/day) and cyclophosphamide (50 mg/day). Patients were treated continuously

Table 1. Patient characteristics at baseline

Patient characteristics	Median (range) or *n* (%)
Number of patients	57
Age (years)	71 (49–90)
Pre-treatment PSA (ng/ml)	27.7 (1.9–7176.0)
Duration of response to initial hormonal treatment (months)	16 (4–94)
ECOG performance status	
0	37 (65)
1	16 (28)
2	4 (7)
Gleason's score of primary tumor	
≤7	11 (19)
8	8 (14)
≥9	27 (47)
Unknown	11
Metastatic disease site	
Bone	47 (82)
Lymph node	8 (14)
Liver	1 (2)
Biologic failure (PSA)	8 (14)
Bone pain	
Present	16 (28)
Absent	41 (72)

PSA, prostate-specific antigen; ECOG, Eastern Cooperative Oncology Group.

Table 2. Prior treatments

Prior therapies ($n = 57$)	n (%)
Primary hormonal therapy	
LHRH analogue plus other hormonal agents[a]	55 (96)
Castration plus other hormonal agents[a]	2 (4)
Prior use of antiandrogen	57 (100)
Prior use of estrogen	4 (7)
Local therapy	
Radical prostatectomy	4 (7)
Radiotherapy	10 (18)
Both	2 (4)
Others	1 (2)
None	40 (70)
Prior chemotherapy	
Estramustine alone	7 (12)
Dexamethasone alone	10 (18)
Estramustine and dexamethasone	13 (23)
Cyclophosphamide, UFT and estramustine	4 (7)
Docetaxel, estramustine and dexamethasone	2 (4)

LHRH, luteinizing hormone-releasing hormone; UFT, uracil plus tegafur.
[a]Other hormonal agents included antiandrogen and estrogen.

until disease progression or unacceptable toxicity. The treatment was reintroduced after complete recovery from toxicity. All patients receiving an LHRH analogue continued the therapy.

Assessability, Toxicity and Response Criteria

Patients underwent a physical examination and laboratory studies including complete blood cell counts, blood chemistry and PSA levels at a minimum of every 4 weeks. The primary endpoint was the proportion of patients with a decline of $\geq$50% in their PSA level. PSA progression was defined by the Prostate Cancer Clinical Trials Working Group 2 criteria (23). In brief, PSA response duration was assessed from the start of therapy to the date of PSA progression, which was defined as a 'PSA increase $\geq$25% and 2 ng/ml above the nadir, and which was confirmed by a second value 3 or more weeks later' for patients with PSA decline from baseline or 'PSA progression $\geq$25% and 2 ng/ml' for patients with no PSA decline from baseline. A 'waterfall plot' was provided for the maximum decline in PSA that occurs at any point after treatment with dexamethasone, UFT and cyclophosphamide for each patient. Increases in PSA levels of >100% were capped at 100%.

Patients with measurable disease as assessed by CT scan and/or MRI were evaluated according to the Response Evaluation Criteria in Solid Tumours criteria if the radiographic images were available. Symptomatic status corresponding to the date of the best PSA response was employed to evaluate symptomatic responses with respect to bone pain. Because we did not employ a formal pain scale assessment, the bone pain response was evaluated by analgesic dose and categorized as improved (defined as a decreased dose), stable (defined as the same dose) or progression (defined as an increased dose) when compared with analgesic administered at the start of therapy.

Toxicities were graded according to the National Cancer Institute Common Toxicity Criteria, version 3.0, and were assessed every 4 weeks based on medical history, physical examination and laboratory studies. Dose reduction or discontinuation of this therapy was employed if a serious adverse effect developed.

The time to PSA progression and survival were calculated using the Kaplan–Meier method and comparisons were made using the log-rank test. Associations between pre- or post-treatment parameters and post-treatment PSA declines were evaluated using a Mann–Whitney U-test. A P value of <0.05 was considered statistically significant. All statistical analyses were performed using SPSS software.

RESULTS

Clinical Response

Thirty-six (63%) of 57 patients showed a PSA decline of $\geq$50%. Figure 1 shows the maximum percent decrease in PSA levels with the combination therapy of dexamethasone, UFT and cyclophosphamide. The median follow-up from the start of this therapy was 19.6 months (range, 2.4–84.4 months). Of 57 patients, 48 (84%) patients showed disease progression (PSA progression or objective progression), whereas 9 patients (16%) were on follow-up with a continued response (median, 19.6 months; range, 2.4–42.7 months). The median time to PSA progression for the entire cohort was 7.2 months (95% confidence interval, 4.1–10.1) as shown in Fig. 2. In patients with a PSA decline of $\geq$50%, the median time to progression was 13.3 months (95% confidence interval, 8.9–20.1). To determine any predictors of a

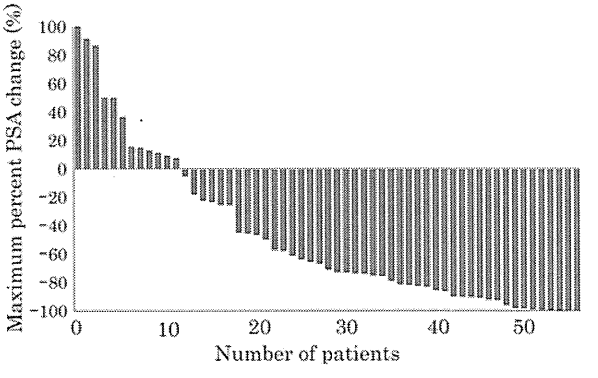

Figure 1. Waterfall plot showing the maximal prostate-specific antigen (PSA) post-therapy change from baseline.

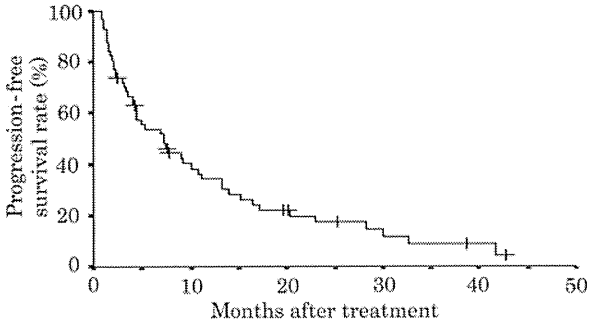

Figure 2. Time to PSA progression for the combination therapy of dexamethasone, uracil plus tegafur and cyclophosphamide.

better time to PSA progression, pre-treatment factors at baseline (age, pre-treatment PSA, duration of response to initial hormonal treatment, ECOG performance status, Gleason's score of the primary tumor and bone pain) were examined, as shown in Table 3. The duration of response to initial hormonal treatment was associated with the time to PSA progression ($P = 0.045$). Pre-treatment PSA, ECOG performance status and Gleason's score of the primary tumor were not statistically significant predictors.

Among 26 patients with prior use of estramustine-based chemotherapies, 14 (54%) showed a PSA decline of $\geq$50%. One of two patients with prior use of docetaxel showed a PSA decline of $\geq$50%. Among 25 patients with prior use of low doses of oral dexamethasone, 10 (40%) showed a PSA decline of $\geq$50% with a median time to progression of 11.1 months (95% confidence interval, 2.3–28.2).

After failure of this therapy, 30 (63%) of 48 patients received docetaxel-based chemotherapy. Eighteen of the 28 evaluable patients (64%) showed a $\geq$50% decrease in PSA levels with docetaxel-based chemotherapy. Two patients were not evaluable due to insufficient PSA data. The median survival after initiation of docetaxel-based chemotherapy was 17 months (95% confidence interval, 7.9–24.1). The median treatment duration of docetaxel-based chemotherapy was 9 months (range, 0.7–51.8 months) and 14 (47%) of 30 patients showed adverse events of Grade 3 or 4, including 7 (23%) patients of neutropenia, 5 (17%) patients of anemia, 4 (13%) patients of infection, 1 (3%) patient of anorexia, 1 (3%) patient of fatigue and 1 (3%) patient of nail change.

Objective responses for measurable lymph node metastasis were assessable in seven patients. Among three patients with a PSA decline of $\geq$50%, two patients showed partial responses and one showed stable disease. Among four patients with a PSA decline of $<$50%, four showed stable disease. Table 4 gives an assessment of bone pain based on PSA decline. Among 16 patients with symptomatic bone metastases, 11 (69%) had improvement and in 5 patients (31%), the pain became stable. Nine of 10 patients with a PSA decline of $\geq$50% showed improvement in bone pain, whereas only 2 of 6 patients with a PSA decline of $<$50% showed improvement. Symptomatic responses of bone metastases were correlated with declines in serum PSA levels of $\geq$50% ($P = 0.017$).

Table 3. Univariate analysis of predictors of time to PSA progression

Patient characteristic	*n*	Median progression-free period (months)	95% CI	*P* value
Age (years)				
≤70	25	8.9	5.2–12.7	0.481
≥71	32	4.5	0.5–8.5	
Pre-treatment PSA				
<Median	28	7.3	1.1–13.5	0.543
≥Median	29	5.3	1.4–9.1	
Duration of response to initial hormonal treatment				
<Median	29	5	0.7–9.3	0.045
≥Median	28	8.9	5.7–12.2	
ECOG performance status				
0	37	8.9	5.2–12.7	0.124
1 or 2	20	4.4	1.1–7.7	
Gleason's score of primary tumor				
≤7	11	4.3	1.5–7.2	0.843
≥8	35	6.9	3.1–10.8	
Bone pain				
Present	16	5.0	3.4–6.7	0.353
Absent	41	7.3	4.4–10.3	

CI, confidence interval.

Table 4. Assessment of bone pain stratified by PSA decline

PSA decline	Bone pain ($n = 16$)		*P* value
	No. of patients		
	Improvement	Stability	
Decline of ≥50%	9	1	0.017
Decline of <50%[a]	2	4	
Total (%)	11 (69)	5 (31)	

[a]The row includes the number of patients with an elevation in their prostate-specific antigen level.

Toxicity

The median duration of continuous full-dose treatment was 18 weeks (range, 1–183 weeks). In 21 (37%) of 57 patients, dose reduction or discontinuation of UFT and/or cyclophosphamide was employed 1–60 weeks (median, 9 weeks) after initiating therapy due to moderate toxicities. The full-dose therapy was then resumed in three patients after recovery. Dexamethasone was continued in all patients until

Table 5. Summary of treatment-related adverse events ($n = 57$)

Adverse events	Number of patients (%)		
	Grade 1 or 2	Grade 3	Grade 4
Neutropenia	10 (18)	2 (4)	1 (2)
Anemia	4 (7)		
Thrombocytopenia	3 (5)		
Anorexia	10 (18)		
Fatigue	9 (16)		
Hypercholesterolemia	4 (7)		
Rash	3 (5)		
Hematuria	2 (4)		
Alopecia	2 (4)		
Peripheral edema	2 (4)		
Hepatic (AST, ALT)	2 (4)		
Diabetes	1 (2)		
Diarrhea	1 (2)		

AST, aspartate aminotransferase; ALT, alanine aminotransferase.

disease progression or treatment failure. Adverse events are shown in Table 5. Most adverse events were mild and manageable on an outpatient basis. Only three (5%) patients showed neutropenia of Grade 3 or higher after 6–20 weeks (median, 7 weeks) of initiating therapy.

DISCUSSION

In the current study, we retrospectively examined the efficacy of an oral combination of dexamethasone, UFT and cyclophosphamide in the treatment of patients with HRPC.

Corticosteroids have long been recognized as active agents in the treatment of HRPC. Several types of glucocorticoids have been used in different doses for clinical trials examining HRPC. A study suggested that dexamethasone shows significantly greater activity in HRPC, in terms of PSA responses, compared with other corticosteroids such as prednisolone or hydrocortisone (11). In our previous report that examined low doses of oral dexamethasone (0.5–2 mg/day) in patients with HRPC, 23 (62%) of 37 patients showed a PSA decline of $\geq$50% (7). In several other trials of low doses of oral dexamethasone, 28–61% of those with HRPC patients showed a PSA decline of $\geq$50% with mild adverse events (6,8–11). The palliation of pain from bone metastases was also reported. To summarize the trials examining low doses of oral dexamethasone in patients with HRPC, symptomatic responses of bone metastases were observed in 43–63% of patients (6–10) and correlated with declines in the serum PSA level of $\geq$50% (7,9,10).

Dexamethasone is often used as a premedication prior to docetaxel-based chemotherapy (4,5). The extent to which dexamethasone might contribute to the efficacy of chemotherapy has been speculated. In a previous report, high doses of dexamethasone (20 mg three times daily given for 1 day every 3 weeks) did not significantly contribute to the PSA response rate of docetaxel-based chemotherapy in HRPC (24). A dose-dependent down-regulation in glucocorticoid receptor levels is one possible explanation (13). Furthermore, high doses of dexamethasone possibly produce adverse effects such as Cushing's syndrome. Thus, low doses of dexamethasone are considered desirable for achieving sufficient response duration and minimizing side effects.

The administration of exogenous corticosteroids is known to suppress production of adrenal androgens and this inhibition of adrenal androgen production is assumed to account for the activity seen in the treatment of men with HRPC (12). Furthermore, the *in vitro* and *in vivo* activity of dexamethasone against androgen-independent prostate cancer cell lines has been reported. In our previous study, dexamethasone inhibited the growth of androgen-independent prostate cancer cell lines, possibly through the disruption of the nuclear factor-κB dependent interleukin-6 pathway (13). Dexamethasone has also been reported to suppress tumor-associated angiogenesis and lymphangiogenesis by decreasing vascular endothelial growth factor (VEGF), interleukin-8 and VEGF-C expression through glucocorticoid receptors in androgen-independent prostate cancer cells (14,15). Further research is necessary to clarify the mechanisms underlying dexamethasone activity and to devise rational drug combinations. The toxicity profile of low doses of dexamethasone makes it an attractive candidate for combined therapy.

A review of earlier prospective randomized clinical trials shows that conventional intravenous administration of 5-fluorouracil (5-FU) and cyclophosphamide, both alone or in combination, produces $<$15% objective responses (complete response or partial response) and has considerable toxicity (25,26). UFT is a mixture of tegafur and uracil in a 1:4 ratio and has the important advantage of improved oral bioavailability in comparison to 5-FU. Tegafur is hydroxylated and converted to 5-FU *in vivo* by hepatic microsomal enzymes (17). Uracil inhibits the activity of hepatic dihydropyrimidine dehydrogenase, an enzyme involved in 5-FU catabolism, thereby leading to increased 5-FU levels when tegafur is administered with uracil (17). In several trials of UFT, as a single agent or combined with leucovorin, 15–19% of patients with HRPC showed a PSA decline of $\geq$50% with low toxicity (16,17). Oral cyclophosphamide has been shown to have greater activity against HRPC with less toxicity than intravenous cyclophosphamide. In trials of oral cyclophosphamide, as a single agent or combined with dexamethasone or other agents, 15–68% of patients with HRPC showed a PSA decline of $\geq$50% (18–22,27–30) and symptomatic responses have also been reported (21,28,29). Pre-clinical studies employing low doses of cyclophosphamide have demonstrated surprisingly potent and durable

antitumor effects in many tumor models of human prostate cancer (31,32).

We preferred cyclophosphamide plus UFT because based on our previous experience, both are oral agents with less hematotoxicity (22). Thus, the oral combination of dexamethasone, UFT and cyclophosphamide was selected and expected to have synergistic antitumor activity. Since these drugs cause antitumor effects through different mechanisms, a chemoresistant phenotype is unlikely to be induced by the selection pressure exerted by chemotherapeutic agents. Indeed, our study demonstrates that among the 25 patients previously treated with low doses of oral dexamethasone, 10 (40%) showed a PSA decline of $\geq$50%, which lasted a median of 11.1 months. Further study is required to determine whether this combination therapy is more active than low doses of dexamethasone alone.

In our study, only the duration of response to initial hormonal treatment was associated with the time to PSA progression. Pre-treatment PSA, ECOG performance status and Gleason's score of the primary tumor were not statistically significant predictors possibly because of small sample size.

Docetaxel-based chemotherapy has been reported to induce significant improvement in median survival by about 2 months in Phase III trials, but side effects occurred more often in the docetaxel group (4,5). In the present trial in which an oral combination of dexamethasone, UFT and cyclophosphamide was used, most adverse events were mild and neutropenia of Grade 3 or higher was shown in only three (5%) patients. This therapy could be easily performed on an outpatient basis for those with HRPC.

After failure of this therapy, 30 patients received docetaxel-based chemotherapy and 18 patients showed a PSA decline of $\geq$50%. The median survival after initiation of docetaxel-based chemotherapy was 17 months. The median treatment duration of docetaxel-based chemotherapy was 9 months and 14 (47%) of 30 patients showed adverse events of Grade 3 or 4. In trials of docetaxel-based chemotherapy, about 50% of patients with HRPC have been reported to show a PSA decline of $\geq$50% (4,5) and the median overall survival have been reported 17.5 months (4). Adverse events of Grade 3 or higher have been shown in 56% of patients in the docetaxel group (4). With respect to response rate, survivals and adverse events, this therapy might not deteriorate efficacy or tolerability of subsequent docetaxel-based chemotherapy. Recently, oral combinations of dexamethasone and cyclophosphamide have been reported to have activity in patients with HRPC, even after the failure of docetaxel-based chemotherapy (21,29). In this trial, only two patients received this therapy after failure of docetaxel-based chemotherapy and one patient showed a PSA decline of $\geq$50%. Further study is required to determine the timing of starting this regimen.

The present study has some limitations. Survival benefits could not be assessed because no control group was available in this trial. In addition, the possibility exists that the impact of this therapy on PSA endpoints will not translate into a worthwhile therapeutic effect on clinically meaningful endpoints (33). To evaluate survival benefits, further randomized trials with well-organized protocols would be needed.

In conclusion, 36 (63%) of 57 patients with HRPC showed a PSA decline of $\geq$50% after treatment with an oral combination of dexamethasone, UFT and cyclophosphamide and the median time to progression was 7.2 months. Symptomatic responses of bone metastases were also proposed and correlated with declines in serum PSA levels of $\geq$50%. This treatment is a completely oral regimen and most adverse events were mild. This regimen may be a useful treatment option before or after docetaxel-based chemotherapy against HRPC.

Conflict of interest statement

None declared.

References

1. Jemal A, Siegel R, Ward E, Hao Y, Xu J, Murray T, et al. Cancer statistics, 2008. *CA Cancer J Clin* 2008;58:71–96.
2. Crawford ED, Eisenberger MA, McLeod DG, Spaulding JT, Benson R, Dorr FA, et al. A controlled trial of leuprolide with and without flutamide in prostatic carcinoma. *N Engl J Med* 1989;321:419–24.
3. Eisenberger MA, Blumenstein BA, Crawford ED, Miller G, McLeod DG, Loehrer PJ, et al. Bilateral orchiectomy with or without flutamide for metastatic prostate cancer. *N Engl J Med* 1998;339:1036–42.
4. Petrylak DP, Tangen CM, Hussain MH, Lara PN, Jr, Jones JA, Taplin ME, et al. Docetaxel and estramustine compared with mitoxantrone and prednisone for advanced refractory prostate cancer. *N Engl J Med* 2004;351:1513–20.
5. Tannock IF, de Wit R, Berry WR, Horti J, Pluzanska A, Chi KN, et al. TAX 327 Investigators. Docetaxel plus prednisone or mitoxantrone plus prednisone for advanced prostate cancer. *N Engl J Med* 2004;351:1502–12.
6. Storlie JA, Buckner JC, Wiseman GA, Burch PA, Hartmann LC, Richardson RL. Prostate specific antigen levels and clinical response to low dose dexamethasone for hormone-refractory metastatic prostate carcinoma. *Cancer* 1995;76:96–100.
7. Nishimura K, Nonomura N, Yasunaga Y, Takaha N, Inoue H, Sugao H, et al. Low doses of oral dexamethasone for hormone-refractory prostate carcinoma. *Cancer* 2000;89:2570–6.
8. Saika T, Kusaka N, Tsushima T, Yamato T, Ohashi T, Suyama B, et al. Treatment of androgen-independent prostate cancer with dexamethasone: a prospective study in stage D2 patients. *Int J Urol* 2001;8:290–4.
9. Morioka M, Kobayashi T, Furukawa Y, Jo Y, Shinkai M, Matsuki T, et al. Prostate-specific antigen levels and prognosis in patients with hormone-refractory prostate cancer treated with low-dose dexamethasone. *Urol Int* 2002;68:10–5.
10. Akakura K, Suzuki H, Ueda T, Komiya A, Ichikawa T, Igarashi T, et al. Possible mechanism of dexamethasone therapy for prostate cancer: suppression of circulating level of interleukin-6. *Prostate* 2003;56:106–9.
11. Venkitaraman R, Thomas K, Huddart RA, Horwich A, Dearnaley DP, Parker CC. Efficacy of low-dose dexamethasone in castration-refractory prostate cancer. *BJU Int* 2007;101:440–3.
12. Khandwala HM, Vassilopoulou-Sellin R, Logethetis CJ, Friend KE. Corticosteroid-induced inhibition of adrenal androgen production in selected patients with prostate cancer. *Endocr Pract* 2001;7:11–5.
13. Nishimura K, Nonomura N, Satoh E, Harada Y, Nakayama M, Tokizane T, et al. Potential mechanism for the effects of

dexamethasone on growth of androgen-independent prostate cancer. *J Natl Cancer Inst* 2001;93:1739–46.
14. Yano A, Fujii Y, Iwai A, Kageyama Y, Kihara K. Glucocorticoids suppress tumor angiogenesis and in vivo growth of prostate cancer cells. *Clin Cancer Res* 2006;12:3003–9.
15. Yano A, Fujii Y, Iwai A, Kawakami S, Kageyama Y, Kihara K. Glucocorticoids suppress tumor lymphangiogenesis of prostate cancer cells. *Clin Cancer Res* 2006;12:6012–7.
16. Miyake H, Hara I, Yamazaki H, Eto H. Clinical outcome of oral uracil/tegafur (UFT) therapy for patients with hormone refractory prostate cancer. *Oncol Rep* 2005;14:673–6.
17. Bhandari MS, Pienta KJ, Fardig J, Olson K, Smith DC. Phase II trial of oral uracil/tegafur plus leucovorin in patients with hormone-refractory prostate carcinoma. *Cancer* 2006;106:1715–21.
18. Nicolini A, Mancini P, Ferrari P, Anselmi L, Tartarelli G, Bonazzi V, et al. Oral low-dose cyclophosphamide in metastatic hormone refractory prostate cancer (MHRPC). *Biomed Pharmacother* 2004;58:447–50.
19. Lord R, Nair S, Schache A, Spicer J, Somaihah N, Khoo V, et al. Low dose metronomic oral cyclophosphamide for hormone resistant prostate cancer: a phase II study. *J Urol* 2007;177:2136–40.
20. Glode LM, Barqawi A, Crighton F, Crawford ED, Kerbel R. Metronomic therapy with cyclophosphamide and dexamethasone for prostate carcinoma. *Cancer* 2003;98:1643–8.
21. Nelius T, Klatte T, de Riese W, Haynes A, Filleur S. Clinical outcome of patients with docetaxel-resistant hormone-refractory prostate cancer treated with second-line cyclophosphamide-based metronomic chemotherapy. *Med Oncol* 2010;27:363–7.
22. Nishimura K, Nonomura N, Ono Y, Nozawa M, Fukui T, Harada Y, et al. Oral combination of cyclophosphamide, uracil plus tegafur and estramustine for hormone-refractory prostate cancer. *Oncology* 2001;60:49–54.
23. Scher HI, Halabi S, Tannock I, Morris M, Sternberg CN, Carducci MA, et al. Prostate Cancer Clinical Trials Working Group. Design and end points of clinical trials for patients with progressive prostate cancer and castrate levels of testosterone: recommendations of the Prostate Cancer Clinical Trials Working Group. *J Clin Oncol* 2008;26:1148–59.
24. Weitzman AL, Shelton G, Zuech N, Owen CE, Judge T, Benson M, et al. Dexamethasone does not significantly contribute to the response rate of docetaxel and estramustine in androgen independent prostate cancer. *J Urol* 2000;163:834–7.
25. Tannock IF. Is there evidence that chemotherapy is of benefit to patients with carcinoma of the prostate? *J Clin Oncol* 1985;3:1013–21.
26. Eisenberger MA, Simon R, O'Dwyer PJ, Wittes RE, Friedman MA. A reevaluation of nonhormonal cytotoxic chemotherapy in the treatment of prostatic carcinoma. *J Clin Oncol* 1985;3:827–41.
27. Daliani DD, Assikis V, Tu SM, Papandreou CN, Pagliaro LC, Holtkamp T, et al. Phase II trial of cyclophosphamide, vincristine, and dexamethasone in the treatment of androgen-independent prostate carcinoma. *Cancer* 2003;97:561–7.
28. Hellerstedt B, Pienta KJ, Redman BG, Esper P, Dunn R, Fardig J, et al. Phase II trial of oral cyclophosphamide, prednisone, and diethylstilbestrol for androgen-independent prostate carcinoma. *Cancer* 2003;98:1603–10.
29. Di Lorenzo G, Autorino R, De Laurentiis M, Forestieri V, Romano C, Prudente A, et al. Thalidomide in combination with oral daily cyclophosphamide in patients with pretreated hormone refractory prostate cancer: a phase I clinical trial. *Cancer Biol Ther* 2007;6:313–7.
30. Fontana A, Galli L, Fioravanti A, Orlandi P, Galli C, Landi L, et al. Clinical and pharmacodynamic evaluation of metronomic cyclophosphamide, celecoxib, and dexamethasone in advanced hormone-refractory prostate cancer. *Clin Cancer Res* 2009;15:4954–62.
31. Man S, Bocci G, Francia G, Green SK, Jothy S, Hanahan D, et al. Antitumor effects in mice of low-dose (metronomic) cyclophosphamide administered continuously through the drinking water. *Cancer Res* 2002;62:2731–5.
32. Shaked Y, Emmenegger U, Francia G, Chen L, Lee CR, Man S, et al. Low-dose metronomic combined with intermittent bolus-dose cyclophosphamide is an effective long-term chemotherapy treatment strategy. *Cancer Res* 2005;65:7045–51.
33. Petrylak DP, Ankerst DP, Jiang CS, Tangen CM, Hussain MH, Lara PN, Jr, et al. Evaluation of prostate-specific antigen declines for surrogacy in patients treated on SWOG 99–16. *J Natl Cancer Inst* 2006;98:516–21.

OPEN ACCESS Freely available online

PLoS one

Androgen-Regulated Transcriptional Control of Sialyltransferases in Prostate Cancer Cells

Koji Hatano[1,2], Yasuhide Miyamoto[3], Masaki Mori[1], Keisuke Nimura[1], Yasutomo Nakai[2], Norio Nonomura[2], Yasufumi Kaneda[1]*

1 Division of Gene Therapy Science, Graduate School of Medicine, Osaka University, Osaka, Japan, **2** Department of Urology, Graduate School of Medicine, Osaka University, Osaka, Japan, **3** Department of Immunology, Osaka Medical Center for Cancer and Cardiovascular Diseases, Osaka, Japan

Abstract

The expression of gangliosides is often associated with cancer progression. Sialyltransferases have received much attention in terms of their relationship with cancer because they modulate the expression of gangliosides. We previously demonstrated that GD1a production was high in castration-resistant prostate cancer cell lines, PC3 and DU145, mainly due to their high expression of β-galactoside α2,3-sialyltransferase (ST3Gal) II (not ST3Gal I), and the expression of both ST3Gals was regulated by NF-κB, mainly by RelB. We herein demonstrate that GD1a was produced in abundance in cancerous tissue samples from human patients with hormone-sensitive prostate cancers as well as castration-resistant prostate cancers. The expression of ST3Gal II was constitutively activated in castration-resistant prostate cancer cell lines, PC3 and DU145, because of the hypomethylation of CpG island in its promoter. However, in androgen-depleted LNCap cells, a hormone-sensitive prostate cancer cell line, the expression of ST3Gal II was silenced because of the hypermethylation of the promoter region. The expression of ST3Gal II in LNCap cells increased with testosterone treatment because of the demethylation of the CpG sites. This testosterone-dependent ST3Gal II expression was suppressed by RelB siRNA, indicating that RelB activated ST3Gal II transcription in the testosterone-induced demethylated promoter. Therefore, in hormone-sensitive prostate cancers, the production of GD1a may be regulated by androgen. This is the first report indicating that the expression of a sialyltransferase is transcriptionally regulated by androgen-dependent demethylation of the CpG sites in its gene promoter.

Citation: Hatano K, Miyamoto Y, Mori M, Nimura K, Nakai Y, et al. (2012) Androgen-Regulated Transcriptional Control of Sialyltransferases in Prostate Cancer Cells. PLoS ONE 7(2): e31234. doi:10.1371/journal.pone.0031234

Editor: Irina Agoulnik, Florida International University, United States of America

Received August 10, 2011; **Accepted** January 4, 2012; **Published** February 8, 2012

Funding: This study was supported by the Program for Promotion of Fundamental Studies in Health Sciences of the National Institute of Biomedical Innovation (Project ID:10-03) and by the Northern Osaka (Saito) Biomedical Knowledge-Based Cluster Creation Project. The funders had no role in study design, data collection and analysis, decision to publish, or preparation of the manuscript.

Competing Interests: The authors have declared that no competing interests exist.

* E-mail: kaneday@gts.med.osaka-u.ac.jp

Introduction

Many cancer cells have aberrant sialylated glycans on their surface. These aberrant molecules may be involved in cancer progression [1–3], but sialylated glycans also play many roles in healthy organisms and non-cancer cells, including embryogenesis, regulation of the immune response and virus binding that leads to infections [4,5]. Sialylated glycans are synthesized by sialyltransferases, which add sialic acids to the oligosaccharide chains of glycoproteins and glycosphingolipids (GSLs) [5]. To date, 20 sialyltransferase genes have been cloned, and the respective enzymes have been grouped into four families according to the carbohydrate linkages they catalyze: β-galactoside α2,3-sialyltransferases (ST3Gal I–VI), β-galactoside α2,6-sialyltransferases (ST6Gal I and II), GalNAc α2,6-sialyltransferases (ST6GalNAc I–VI), and α2,8-sialyltransferases (ST8Sia I–VI) [6]. During neoplastic transformation and cancer progression, the activity of sialyltransferases is often altered, and consequently, cancer cells have more heavily sialylated glycans on their surface than non-cancer cells [1,2,7].

GSLs that contain sialic acids are known as gangliosides and are expressed at high levels in various cancer cells [3]. The gangliosides present on cancer cells are used as biomarkers or treatment targets, and the enriched gangliosides differ between cancer cell types [8–10]. We have focused on GD1a synthesis in cancer cells because GD1a has several biological actions that promote cancer progression. For example, highly metastatic cancer cells have abundant GD1a, and GD1a is involved in cancer cell adhesion to endothelial cells during metastasis [11]. The GD1a shed by tumor cells in the tumor microenvironment promotes angiogenesis and enhances growth factor signaling by increasing the dimerization of growth factor receptors [12–15]. Therefore, GD1a may be involved in cancer cell proliferation and metastasis. Furthermore, this ganglioside is a receptor for the Sendai virus [16], and inactivated Sendai virus particles [hemagglutinating virus of Japan envelope (HVJ-E)] induce apoptosis in several human cancer cells with enriched GD1a on their surface [17]. Therefore, GD1a may be an attractive molecule from the viewpoint of cancer therapy.

GD1a has been reported to be abundantly produced in castration-resistant prostate cancer cells [17–20], and we previously demonstrated that castration-resistant prostate cancer cells were effectively eradicated by HVJ-E [17]. GD1a is synthesized from GM1 by ST3Gal I and II. The Km value of ST3Gal II for GM1 is smaller than that of ST3Gal I; thus, ST3Gal II preferentially contributes to GD1a synthesis [6,21–24]. We

recently demonstrated that abundant production of GD1a in castration-resistant prostate cancer cells is correlated with the high levels of ST3Gal II expression [20] and that ST3Gal II expression is regulated by NF-κB, mainly by RelB, in castration-resistant prostate cancer cells [20]. Although the RelB levels were similar in a hormone-sensitive prostate cancer cell line (LNCap) and castration-resistant prostate cancer cells, and although ST3Gal I was expressed in LNCap cells [20], the expression of ST3Gal II was silenced in LNCap cells, and GD1a was much less abundant in the LNCap cells [17,20].

There has so far been no published analysis of the ganglioside levels in cancerous tissue samples from human patients with prostate cancer; however, an endogenous immune response to GD1a was observed in patients with hormone-sensitive prostate cancer, but not in healthy controls [19], thus suggesting that GD1a is abundantly produced in hormone-sensitive prostate cancers. Prostate cancer exhibits androgen-dependent growth and progression [25]; therefore, androgens may also regulate the GD1a production that is related to cancer progression. However, there have also been no published studies that have examined the hormonal control of sialylated glycan synthesis.

The aim of this study was to determine whether GD1a is produced in abundance in hormone-sensitive prostate cancers in patients and to analyze the transcriptional control of sialyltransferases, especially ST3Gal II, required for the synthesis of GD1a in hormone-sensitive prostate cancers.

Materials and Methods

Ethics statement

Written informed consent was obtained from all patients for the use of their tissue specimens, and the use of such specimens was approved by the Osaka University Hospital Institutional Review Board (Osaka, Japan).

Cell culture

Castration-resistant human prostate cancer cell lines, PC3 and DU145, and a hormone-sensitive human prostate cancer cell line, LNCap clone FGC, were purchased from the American Type Culture Collection (Rockville, MD). A normal human prostatic epithelial cell, PNT2, was purchased from the European Collection of Animal Cell Cultures (Porton Down, UK). PC3 cells were maintained in Dulbecco's modified Eagle F12 medium (Nacalai Tesque, Kyoto, Japan), and DU145, LNCap, and PNT2 cells were maintained in RPMI 1640 medium (Nacalai Tesque, Kyoto, Japan). All media were supplemented with 10% fetal bovine serum (FBS), 100 U/ml penicillin, and 100 μg/ml streptomycin. The cells were incubated at 37°C in a humidified atmosphere of 95% air and 5% CO_2.

Reagents and antibodies

Trichostatin A (TSA) and 5-aza-2′-deoxycytidine (5-azadC) were purchased from Wako Pure Chemical Industries (Osaka, Japan). Testosterone was purchased from Tokyo Chemical Industry (Tokyo, Japan). Bicalutamide was purchased from Enzo Life Sciences (Plymouth Meeting, PA). Restriction enzymes, *Msp*I and *Hpa*II, were purchased from New England Biolabs (Ipswich, MA). Anti-human RelB (C1E4) was purchased from Cell Signaling (Danvers, MA). Anti-human β-actin (AC-15) was purchased from Abcam (Cambridge, UK).

Real-time quantitative RT-PCR

Total RNA was isolated using an RNeasy RNA isolation kit (Qiagen, Valencia, CA). The cDNA was synthesized using a High Capacity cDNA Reverse Transcription Kit (Applied Biosystems, Foster City, CA). Real-time quantitative PCR was performed with an Applied Biosystems 7900 HT Fast Real-Time PCR system under the following conditions: 95°C for 10 min followed by 40 cycles of 95°C for 15 s and 60°C for 1 min. Mixtures of probes and primer pairs specific for human ST3Gal I (Hs00161688_m1), ST3Gal II (Hs00199480_m1), ST3Gal VI (Hs00196086_m1), RelB (Hs00232399_m1), and glyceraldehyde-3-phosphate dehydrogenase (GAPDH) (Hs99999905_m1) were purchased from Applied Biosystems. The relative expression levels were calculated from a standard curve obtained using log dilutions of cDNA containing the gene of interest, and values were normalized to GAPDH, an internal control.

Evaluation using a reporter gene

Genes were transfected into cells along with a luciferase reporter construct driven by a NF-κB binding site, RelA, and RelB (NF-κB luciferase reporter gene; BD Bioscience Clontech, Palo Alto, CA), using the Fugene HD reagent (Roche, Basel, Switzerland). The luciferase activity was measured with the dual-luciferase assay system (Promega, Madison, WI).

Western blot analysis

The cells were harvested and lysed with RIPA lysis buffer. Protein samples were separated by sodium dodecyl sulfate polyacrylamide gel electrophoresis. The separated proteins were transferred onto polyvinylidene fluoride membranes, then the membranes were blocked with 5% skim milk and incubated overnight at 4°C with anti-RelB (1:500) or anti-β-actin (1:2000) antibodies. The membranes were washed and labeled with a 1:2000 dilution of horseradish peroxidase–conjugated secondary antibody (GE Healthcare, Buckinghamshire, UK) at room temperature for approximately 1 hour. Detection by chemiluminescence was performed according to the ECL user's guide (Amersham, Buckinghamshire, UK). Images were captured with ImageQuant LAS 4000mini (GE Healthcare, Buckinghamshire, UK), and quantification of Western blot signals was performed by densitometry with ImageQuant TL software (GE Healthcare, Buckinghamshire, UK).

RNA interference experiments

The following double-strand stealth small interfering RNA (siRNA) oligonucleotides and scrambled RNA were purchased from Invitrogen (Tokyo, Japan): siRNA oligonucleotides against RelB were (sense) 5′-UCUUCAGGGACCCAGCGUUGUAGGG-3′ and (antisense) 5′-CCCUACAACGCUGGGUCCCUGAAGA-3′. Transfections were performed with lipofectamine RNAiMAX (Invitrogen, Tokyo, Japan), according to the manufacturer's instructions.

Methylation-specific PCR (MSP) analysis

DNA methylation was examined at the CpG islands by a MSP analysis as previously reported [26]. For the MSP analysis, genomic DNA was extracted from cells and purified using the QIAamp DNA kit (Qiagen, Valencia, CA). Genomic DNA was subjected to bisulfite conversion using an EZ DNA Methylation Kit (Zymo Research, Irvine, CA). Based on the sequence of the ST3Gal II p1 promoter and ST3Gal I p1 promoter, methylated-specific primers and unmethylated-specific primers were designed using the Methyl Primer Express Software program version 1.0 (Applied Biosystems, Foster City, CA). The ST3Gal II-methylated-specific primers were sense, 5′-TAGGGCGTAGCGGTTTTATC-3′, antisense, 5′-ACTAACCGAAAACGCCTCTC-3′,

and the ST3Gal II-unmethylated-specific primers were sense, 5′-GGTTAGGGTGTAGTGGTTTTATT-3′, and antisense, 5′-CACACTAACCAAAAACACCTCTC-3′. The ST3Gal II 5′-untranslated region from −659 to −495 was chosen for the MSP analysis. The ST3Gal I-methylated-specific primers were sense, 5′-TAGGGTCGGTCGTAGTGTTC-3′, antisense, 5′-ACCGATCCCCTACTAACGAC-3′, and the ST3Gal I-unmethylated-specific primers were sense, 5′-TTAGGGTTGGTTGTAGTGTTT-3′, and antisense, 5′-AACCAATCCCCTACTAACAAC-3′. The ST3Gal I 5′-untranslated region from −697 to −535 was chosen for the MSP analysis. The glutathione S-transferase-π gene (GSTP1) -methylated-specific primers were sense, 5′-AGTTGCGCGGCGATTTC-3′, antisense, 5′-GCCCCAATACTAAATCACGACG-3′, and the GSTP1-unmethylated-specific primers were sense, 5′-GATGTTTGGGGTGTAGTGGTTGTT-3′, and antisense, 5′-CCACCCCAATACTAAATCACAACA-3′, as described previously [27]. Purified genomic DNA treated with sodium bisulfite was amplified by PCR as follows: 2 min at 95°C for denaturation, 35 cycles of amplification (95°C for 30 s, 56°C for 30 s, and 72°C for 30 s). Human genomic DNA or enzymatically methylated human genomic DNA (Chemicon International, Temecula, CA) was bisulfite-converted and used as a positive control for the unmethylated or methylated genes. The absence of a DNA template served as a negative control. The products were analyzed in 2% agarose gels stained with ethidium bromide.

Isolation of acidic GSLs from prostate cancer tissues

Patients diagnosed with prostate cancer had undergone prostate biopsy or resection of tumors at Osaka University Hospital (Osaka, Japan). Primary cancerous tissue samples were frozen in liquid nitrogen and stored at −80°C until use. The majority of the experimental procedures have been reported previously [28]. In brief, the samples were homogenized in chloroform/methanol (2:1, v/v), and incubated at room temperature for 2 h with 30 s of sonication every 30 min. Methanol was then added to the samples, which were centrifuged at 1800×g for 15 min. The pellets were homogenized in chloroform/methanol/water (1:2:0.8, v/v/v), incubated at room temperature for 2 h, and then centrifuged at 1800×g for 15 min. Both extracts were combined and evaporated to dryness in a vacuum concentrator. The residue was dissolved in chloroform/methanol/water (30:60:8) and fractionated by DEAE–Sephadex A25 column chromatography to separate neutral GSLs from acidic GSLs.

Analysis of acidic GSLs

The structures of the acidic GSLs were analyzed by enzymatic release of carbohydrate moieties, fluorescent labeling with aminopyridine, and two-dimensional mapping followed by mass spectrometry. The majority of experimental procedures have been reported previously [28]. In brief, the acidic GSLs were extracted from primary cancer tissue samples or cultured cancer cells and digested with recombinant endoglycoceramidase II from *Rhodococcus* sp. (Takara Bio Inc., Shiga, Japan). The released oligosaccharides were labeled with 2-aminopyridine (2-AP) and separated on a Shimadzu LC-20A HPLC system (Shimadzu Corporation, Kyoto, Japan) equipped with a Waters 2475 fluorescence detector. Normal-phase HPLC was performed on a TSK gel Amide-80 column (0.2×25 cm, Tosoh, Tokyo, Japan). The molecular size of each pyridylaminated (PA)-oligosaccharide is given in glucose units (Gu) based on the elution times of PA-isomaltooligosaccharides. Reversed-phase HPLC was performed on a TSK gel ODS-80Ts column (0.2×15 cm, Tosoh). The retention time of each PA-oligosaccharide is given in glucose units based on the elution times of the PA-isomaltooligosaccharides. Therefore, the behaviors of a given compound in these two columns provide a unique set of Gu (amide) and Gu (ODS) values, which correspond to coordinates on a 2-D map. PA-oligosaccharides were analyzed by LC/ESI MS/MS. Standard PA-oligosaccharides, PA-GM1 and PA-GD1a, were purchased from Takara Bio, and PA-LST-a and PA-SPG were isolated as in our previous study [28].

Statistical analyses

The results are reported as the means ± standard error (S.E.). The two-tailed unpaired Student's *t*-test was used to determine the statistical significance of the differences between two groups. Probability values of $P<0.05$ were considered to be statistically significant. The statistical analysis was performed using the StatView 5.0 software program (SAS Institute, Cary, NC).

Results

Analyses of gangliosides in cancerous tissue samples from patients with prostate cancer

We previously demonstrated that GD1a was abundant in castration-resistant prostate cancer cell lines (including PC3 and DU145), while it was barely detectable in a hormone-sensitive prostate cancer cell line (LNCap) and a normal prostate epithelial cell line (PNT2) [17]. We examined the levels of gangliosides in samples of cancerous tissue from eight patients with prostate cancer, including six patients with advanced hormone-sensitive prostate cancer and two patients with castration-resistant prostate cancer (Table 1). The acidic GSLs extracted from cancerous tissue samples from these patients were examined using HPLC (Fig. 1). Both GM3 and GD3 are common gangliosides expressed in both prostate cancer cells and normal prostate epithelial cells [18,19]. GD1a was produced in the cancerous tissue samples from both the patients with hormone-sensitive prostate cancers and those with castration-resistant prostate cancers (Fig. 1A, 1B). In all of the patient' samples (hormone-sensitive and castration-resistant), the mean percentage of total acidic GSLs with GD1a was 8.1%, and no statistically significant difference was seen compared with the value from castration-resistant prostate cancer cell lines (PC3 and DU145) (Fig. 1C).

Androgen-dependent regulation of ST3Gal II in LNCap cells

The synthesis of GD1a is mainly regulated by ST3Gal II, and the expression of ST3Gal II is regulated by NF-κB, mainly by

Table 1. Patient characteristics.

Patient	Site	HS/CR	PSA	Gleason sum
1	Prostate/Bone metastasis	HS	706	8
2	Prostate	HS	914	9
3	Prostate	HS	2800	9
4	Prostate	HS	3.1	9
5	Prostate	HS	639	9
6	Prostate	HS	2296	9
7	Prostate	CR	36	-
8	Prostate	CR	6.2	-

HS, Hormone-sensitive; CR, Castration-resistant.
doi:10.1371/journal.pone.0031234.t001

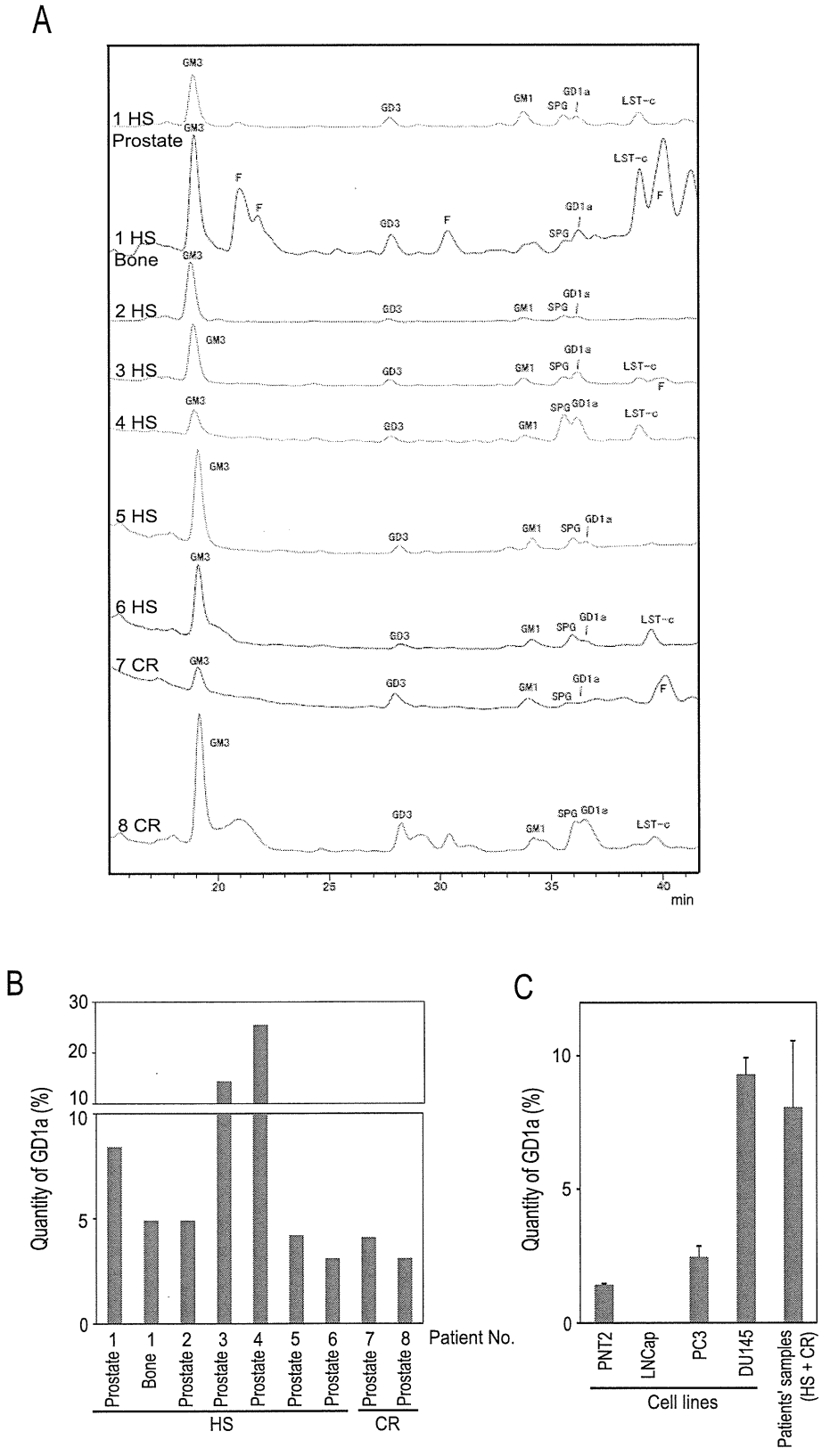

Figure 1. The results of the analyses of gangliosides in cancerous tissue samples from human prostate cancer patients. (A) The acidic GSLs from the cancerous tissue samples from eight patients with prostate cancer, including six patients with advanced hormone-sensitive prostate cancer and two patients with castration-resistant prostate cancer were separated by the molecular size of the oligosaccharides using normal-phase

HPLC. Samples from one patient (designated Case 1) were taken from both the prostate and bone metastases for evaluation. (B) The acidic GSLs in the primary cancerous tissue samples were separated by the molecular size of the oligosaccharides using HPLC. The quantity of GD1a is presented as a percentage of the total acidic GSLs with GD1a. (C) The acidic GSLs in cultured prostate cancer cells were separated by the molecular size of the oligosaccharides using HPLC. The assay was done in triplicate, and the means ± S.E. GD1a levels are shown as the ratio to the total acidic GSLs in the cell lines. The mean ± S.E. GD1a level was also presented as the ratio to the total acidic GSLs in the patients' samples (HS+CR) indicated in Figure 1B. (HS, hormone-sensitive; CR, castration-resistant; F, free glycan).
doi:10.1371/journal.pone.0031234.g001

RelB, in castration-resistant prostate cancer cell lines [20]. The amounts of nuclear RelB were similar in hormone-sensitive LNCap cells and castration-resistant PC3 and DU145 cells [20], but the expression of ST3Gal II was lower in the LNCap cells than in the PC3 and DU145 cells [20].

The LNCap cell culture medium is routinely supplemented with 10% fetal bovine serum (FBS). A recent report showed that media supplemented with 10% FBS contains only castrate levels of testosterone [29]; in contrast, hormone-sensitive prostate cancers of untreated patients usually grow in an environment containing testosterone *in vivo*. To analyze the transcriptional control of ST3Gal II in hormone-sensitive prostate cancers, we examined whether the expression of ST3Gal II was controlled by testosterone in LNCap cells. LNCap cells were treated with testosterone (0–1000 nM), and were incubated for 120 h. The quantitative real-time PCR analyses showed that the expression of ST3Gal II was higher in LNCap cells treated with testosterone than in the LNCap cells that were not (Fig. 2A). Furthermore, the induction of ST3Gal II after testosterone treatment was suppressed by an anti-androgen, bicalutamide, in LNCap cells (Fig. 2B). To ensure that there were no androgens present in the media, LNCap cells were incubated in charcoal-stripped serum for 48 h. The basal level of ST3Gal II was not significantly different between the 10% FBS- and charcoal stripped serum-supplemented LNCap cells (Fig. 2C). The LNCap cells were subsequently treated with 100 nM testosterone, and the time-course of expression following testosterone treatment was evaluated. The expression of ST3Gal II was increased 48 h after testosterone treatment, and remained elevated for more than 120 h in the LNCap cells (Fig. 2C). To evaluate the NF-κB activity after testosterone treatment, LNCap cells were transfected with an NF-κB luciferase reporter construct and incubated for 120 h with or without testosterone. The NF-κB activity was not significantly different in the testosterone-treated LNCap cells compared to the cells cultured without testosterone (Figure S1). In PC3 and PNT2 cells, no significant increase in the expression of ST3Gal II was detected regardless of whether the cells cultured with or without testosterone (Fig. 2A). The expression of ST3Gal II did not increase after testosterone treatment in the PC3 cells at any time point up to 120 h (Figure S2). Based on these findings, we hypothesized that the media with castrate levels of testosterone led to the epigenetic silencing of ST3Gal, a gene required for the synthesis of GD1a, in LNCap cells.

Epigenetic regulation of ST3Gal II in LNCap cells

Next, we examined whether ST3Gal II was epigenetically regulated in LNCap cells. The LNCap cells were treated with a DNA methyltransferase inhibitor, 5-azadC, and incubated for 120 h (Fig. 3A). The quantitative real-time PCR analyses showed that the expression of ST3Gal II was up-regulated after 5-azadC treatment. Following this experiment, the LNCap cells were treated with a histone deacetylase inhibitor, TSA, and incubated for 48 h (Fig. 3B). The quantitative real-time PCR analyses showed that the expression of ST3Gal II was up-regulated after TSA treatment. These results suggest that epigenetic regulation, including DNA methylation and histone modifications, may be involved in the repression of the ST3Gal II gene in LNCap cells. In further experiments, we focused on DNA methylation at the CpG island in the ST3Gal II promoter.

Control of DNA methylation at the CpG island in the ST3Gal II gene promoter in prostate cancer cells

The gene for human ST3Gal II has been cloned, and the p1 promoter is reportedly necessary for active transcription of this gene in prostate cancer cells [30]. The ST3Gal II promoter sequences are publically available, and we identified a CpG island in the ST3Gal II p1 promoter using the Methyl Primer Express Software program, version 1.0 (Applied Biosystems, Foster City, CA) (Fig. 4A). We examined the methylation at the CpG in the ST3Gal II promoter using the MSP analysis. Genomic DNA was isolated from LNCap cells treated with or without 5-azadC for 120 h, that were then treated with sodium bisulfite, and the DNA was amplified with primers specific for the unmethylated or the methylated ST3Gal II promoter (Fig. 4B). In LNCap cells, the CpG island in the ST3Gal II promoter, which was originally hypermethylated, was demethylated by 5-azadC treatment. Next, we examined the effect of testosterone on the methylation at the CpG in the ST3Gal II promoter in LNCap cells using a MSP analysis (Fig. 4C). In the PC3 and DU145 cells, the CpG island of the ST3Gal II promoter was constitutively hypomethylated. In the LNCap cells, the CpG island of the ST3Gal II promoter was hypermethylated in the absence of testosterone and demethylated in the presence of testosterone. Furthermore, the demethylation at the CpG island in the ST3Gal II promoter after testosterone treatment was suppressed by an anti-androgen, bicalutamide, in LNCap cells (Fig. 4D).

We also examined whether global DNA demethylation is under androgen-dependent control in LNCap cells. We examined the overall restriction patterns of *Msp*I- or *Hpa*II-digested genomic DNA. These enzymes are isoschizomers that recognize the target sequence 5′-CCGG-3′, but the activity of *Hpa*II is inhibited by methylation of the inner cytosine of this sequence. The genomic DNA isolated form LNCap cells treated with or without testosterone was digested using *Msp*I or *Hpa*II (Figure S3A). Testosterone treatment did not greatly affect the digestion pattern of *Hpa*II-treated genomic DNA from LNCap cells, indicating that global DNA demethylation in LNCap cells was not under androgen-dependent control. We then examined the CpG island of GSTP1, which is reported to be hypermethylated during prostate carcinogenesis and also in LNCap cells [27]. Based on the MSP analysis, testosterone treatment did not affect the methylation of GSTP1 in LNCap cells (Figure S3B). Thus, the androgen-dependent control of DNA demethylation may be induced preferentially at the CpG island in the ST3Gal II gene promoter in LNCap cells.

Androgen-dependent and epigenetic regulation of ST3Gal I in LNCap cells

Although GD1a is synthesized from GM1 mainly by ST3Gal II, ST3Gal I may also contribute to the synthesis of GD1a [6,21–24]. We previously reported that ST3Gal I was expressed in LNCap cells, while the expression of ST3Gal II was silenced [20].

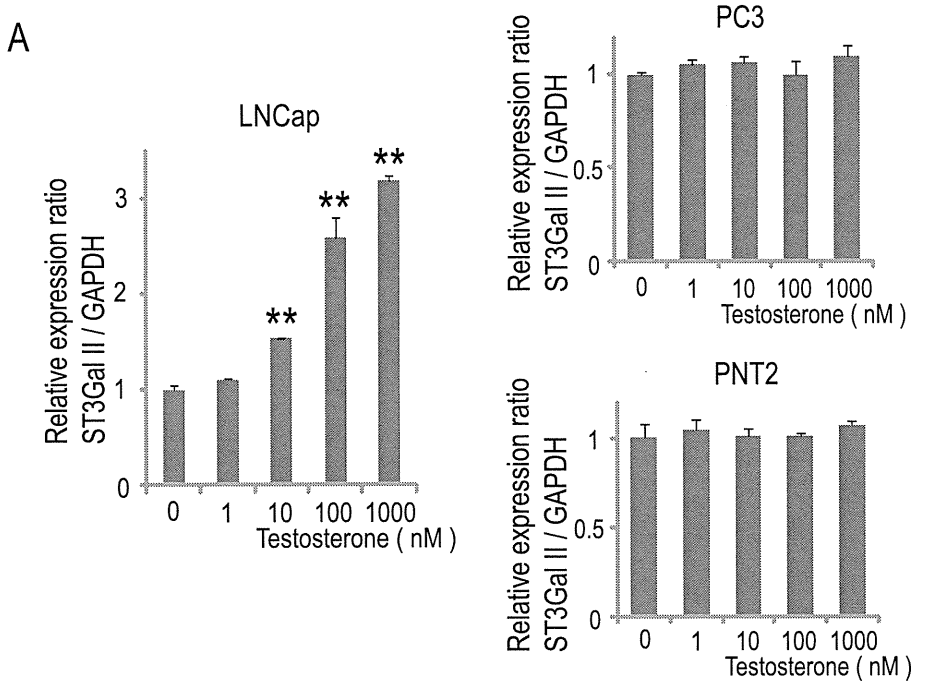
A
LNCap
Relative expression ratio
ST3Gal II / GAPDH
0
1
2
3
**
**
**
0 1 10 100 1000
Testosterone (nM)
PC3
Relative expression ratio
ST3Gal II / GAPDH
0
0.5
1
0 1 10 100 1000
Testosterone (nM)
PNT2
Relative expression ratio
ST3Gal II / GAPDH
0
0.5
1
0 1 10 100 1000
Testosterone (nM)

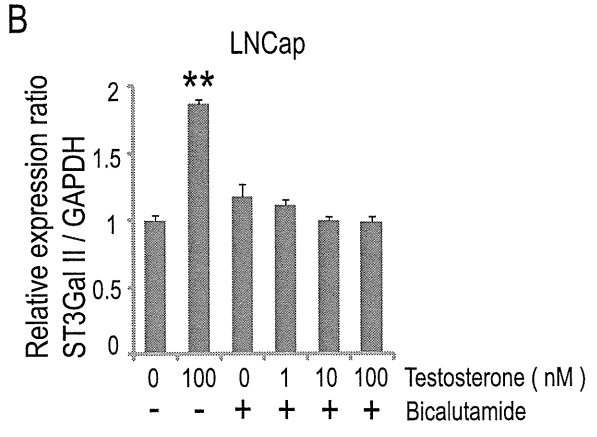
B
LNCap
Relative expression ratio
ST3Gal II / GAPDH
0
0.5
1
1.5
2
**
0 100 0 1 10 100 Testosterone (nM)
- - + + + + Bicalutamide

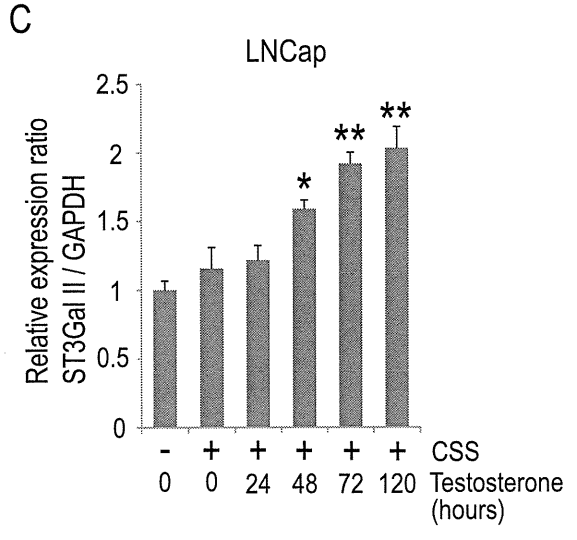
C
LNCap
Relative expression ratio
ST3Gal II / GAPDH
0
0.5
1
1.5
2
2.5
*
**
**
- + + + + + CSS
0 0 24 48 72 120 Testosterone
(hours)